FEDERAL UNIVERSITY OF TECHNOLOGY

POST-GRADUATE PROGRAM IN MATERIALS SCIENCE AND ENGINEERING

ARIEL COLAÇO DE OLIVEIRA

DISSERTATION

LONDRINA

2018

ARIEL COLAÇO DE OLIVEIRA

Preparation, characterization, and scaffolding capacity of chitosan/gellan gum-based hydrogel assemblies

Master's dissertation presented as a prerequisite for obtaining a master's degree in Materials Science and Engineering from the Post-Graduate Program in Materials Science and Engineering (PPGCEM) at Federal University of Technology - UTFPR, Londrina Campus.

Advisor: Prof. Dr. Alessandro Francisco Martins

Co-advisor: Prof. Dr. Bruno Henrique Vilsinski

LONDRINA

2018

Dados Internacionais de Catalogação na Publicação (CIP)
Biblioteca UTFPR - Câmpus Londrina

O48p Oliveira, Ariel Colaço de
Preparation, characterization, and scaffolding capacity of chitosan / gellan gum-based hydrogel assemblies / Ariel Colaço de Oliveira. - Londrina : [s.n.], 2018.
69 f. : il. ; 30 cm.

Orientador: Prof. Dr. Alessandro Francisco Martins
Coorientador: Prof. Dr. Bruno Henrique Vilsinski
Dissertação (Mestrado) - Universidade Tecnológica Federal do Paraná. Programa de Pós-Graduação em Ciência e Engenharia de Materiais. Londrina, 2018.
Bibliografia: f. 62-69.

1. Polímeros. 2. Polissacarídeos. 3. Biocompatibilidade. 4. Células-tronco. 5. Engenharia biomédica. I. Martins, Alessandro Francisco, orient. II. Vilsinski, Bruno Henrique, coorient. III. Universidade Tecnológica Federal do Paraná. IV. Programa de Pós-Graduação em Ciência e Engenharia de Materiais. V. Título.

CDD: 620.11

Ficha catalográfica elaborada por Cristina Benedeti Guilhem - CRB: 9/911

Ministry of Education

Federal University of Technology

Pro-Rectory of Research and Graduate Studies
Materials Science and Engineering from the Post-Graduate
Program in Materials Science and Engineering (PPGCEM)
Campus Londrina

UNIVERSIDADE TECNOLÓGICA FEDERAL DO PARANÁ

TERM OF APPROVAL

Preparation, characterization, and scaffolding capacity of chitosan/gellan gum-based hydrogel assemblies

by

ARIEL COLAÇO DE OLIVEIRA

Dissertation presented on December 7, 2018, as a partial requirement to obtain the title of MASTER in MATERIALS SCIENCE AND ENGINEERING by the Post-Graduate Program in Materials Science and Engineering (PPGCEM), FEDERAL UNIVERSITY OF TECHNOLOGY at Paraná (UTFPR) – Londrina Câmpus. The candidate was indicted by the Examining Bank composed of the Teachers, as listed below. After deliberation, the Examining Board considered the work APPROVED.

_____
Orientador: Prof. Dr. Alessandro Francisco Martins
UTFPR – Campus Apucarana

_____
Prof. Dr. Adley Forti Rubira (Membro titular)
UEM – Universidade Estadual de Maringá

_____
Prof. Dr Renato Márcio Ribeiro Viana (Membro titular)
UTFPR – Campus Londrina

_____
Prof. Dr. Carlos Eduardo Cava
Coordinator of the Post-Graduate Program in Materials Science and Engineering
UTFPR – Campus Londrina

* The signed Approval Sheet is in the Coordination of the Master's Program in Materials Science and Engineering.

[30] Young men will be wary and weary, and young men will surely fall.
[31] But they that wait on the Lord shall renew their strength; they shall mount up with wings like eagles; they shall run, and not be weary; they shall walk, and not faint.

Isaias 40: 30-31

THANKS

I thank God for the opportunity to learn on difficulties and, then to be here to complete more one step in my life.

In particular, I want to thank my grandmother Dona Zoraide (*in memoriam*) because she has created me, gave me love and she always cared about me. Without her, I would not be here and I would not be this person that I became. I'm flattered to be able to thank her; however; this is the only thing that I can do for her. At this moment, I would like to see her more once and then she could watch this moment.

My Father Elson, my Mother Aparecida, my Sister Laura and especially my Brother Felipe. Felipe was always by my side, helping me and supporting me, especially in the studies. I can sure say; I am here because of you.

To thank Joaquim, Lu, Juliano, Guete, Daiane, Peba, Anderson, Denis, Bari, Testão, Diego (zebra), Felipe (Oliver), Leandro (Popó), Augusto and other friends that I do not remember at this moment. This victory depended on all of them because they have shared your victories with me when my family was not present.

To thank Father Je and his family, who have given me support since I arrived in Apucarana city. God has put this new family in my way to help me, guide me and teach me. I am very grateful to know this family, my second family.

To thank Leandro, Ariana and Santa Cruz do Rio Pardo's family because they gave me help when I needed a refuge. I am very grateful to everyone.

To thank my Uncle Colaço since he was a child, he taught us to be men. He has helped me since I was a child, not only executing his role as an uncle but as a father.

To thank Aunt Nilse because she has been like a mother, and always she advised me to study. I write in remembrance of your aunt smile and I only have words of thanks. Thank you, my dear.

To thank my mentor and friend Professor Alessandro Francisco Martins, in which he always supported and believed me, making possible the realization of this dream.

To thank Professor Elton G. Bonafé, Johny P. Monteiro and Sandor Venter, for their patience, teachings and especially for showing me that the way is arduous but achievable.

To thank Glayce for the help and companionship these last months. Helping me daily. Thank you, my dear.

To thank my friends and colleagues of PPGCEM. I am grateful to all. Among them, Joziel, Fernanda, Débora, Jéssica, Bruno, Rosicler, André, Katlyn, Jessica (Londrina) and all that I do not remember at the time.

ABSTRACT

In this study, we have demonstrated the production and characterization of hydrogels based on chitosan and gellan gum (CS/GG) assemblies. Hydrogels were created without any covalent and metallic crosslinking agents, conventionally used to yield polysaccharide-based hydrogels. Polyelectrolyte complexes (PECs) were characterized by infrared spectroscopy (FTIR), thermal analysis (TGA and DSC), X-ray photoelectron spectroscopy (XPS), scanning electron microscopy (SEM) and wide-angle X-ray scattering (WAXS). Hydrogels containing chitosan (CS) contents ranging from 40 to 80 wt.% were yielded by performing CS/GG blends at 60°C. CS/GG wt.%/wt.% ratio was modulated in the blend to promote hydrogels with interconnected pore networks, structural homogeneity, durability, and hydrophilicity. These properties are required in the development of scaffold-based platforms. The polymer chains in the hydrogel matrices have self-assembled during the neutralization step. The reorganization was confirmed through TGA, DSC, and SEM techniques. A hydrogel prepared from the CS/GG 60/40 ratio (sample CS/GG(60-40)) showed swelling degree (SD%) of 6460% after 4 days in PBS buffer. This PEC had no potential to act as scaffold matrix; however, a cytocompatible CS/GG hydrogel yielded at 80/20 CS/GG ratio (sample CS/GG80-20) supported fixation, growth, and spreading of bone mesenchymal stem cells (BMSCs) after 9 days of cell culture. This hydrogel exhibited desirable properties to be applied in tissue engineering arena.

Keywords: Hydrogels, Self-assembling, Cell Viability, Stem Cells, Cytocompatibility, Biomedical Engineering.

RESUMO

Demonstramos neste estudo à produção e caracterização de hidrogéis físicos termossensíveis a base de quitosana e goma de gelana (CS/GG). Os materiais foram produzidos sem adição de agentes de reticulação covalentes e metálicos, convencionalmente utilizados na produção de hidrogéis a base de polissacarídeos. Os complexos polieletrolíticos (PECs) foram caracterizados por meio de espectroscopia na região do infravermelho (FTIR), análise térmica (TGA e DSC), espectroscopia de fotoelétrons de raios-X (XPS), microscopia eletrônica de varredura (SEM) e difração de raios-X (WAXS). Hidrogéis contendo quitosana (CS), com teor variando de 40 a 80 m.% foram criados a partir de blendas CS/GG obtidas a 60°C. A razão CS/GG m.%/m.% foi modulada na blenda para promover aos hidrogéis morfologia com poros interconectados, homogeneidade estrutural, durabilidade e hidrofilicidade. Estas propriedades são requeridas no desenvolvimento de plataformas *scaffolds*. As cadeias poliméricas dos hidrogéis se reorganizaram durante a etapa de neutralização. A reorganização foi confirmada por meio das técnicas de TGA, DSC, e SEM. O hidrogel preparado a partir da razão CS/GG 60/40 (amostra CS/GG(60-40)) apresentou grau de intumescimento (SD%) de 6460% depois de 4 dias em tampão PBS. Este PEC não apresentou potencial para atuar como matriz scaffold, porém o hidrogel citocompatível produzido na razão CS/GG 80/20 (amostra CS/GG(80-20) com SD = 1813% após 4 dias em PBS) suportou a fixação, proliferação e disseminação de células tronco mesenquimais do tecido ósseo (BMSCs) após 9 dias de cultura celular. Este hidrogel exibiu propriedades desejáveis para ser aplicado na área de engenharia de tecidos.

Palavras-chave: Hidrogéis, Reorganização, Viabilidade Celular, Células Tronco, Citocompatibilidade, Engenharia Biomédica.

173 **INDEX OF FIGURES**

174

LIST OF TABLES

LIST OF ACRONYMS

BMSCs = Bone mesenchymal stem

CS = Chitosan

DSC = Differential scanning calorimeter

ECM = Extracellular membrane matrix

FTIR = Infrared spectroscopy

GG = Gellan gum

PBS = Phosphate-saline buffer at pH 7.4

PEC = Polyelectrolyte complex

PECs = Polyelectrolyte complexes

SEM = Scanning electron microscope

SGF = Simulated gastric fluid

XPS = X-ray photoelectron spectroscopy

TGA = Thermogravimetric analysis

WAXS = Wide-angle X-ray scattering

RESULTS OBTAINED DURING THE MASTER COURSE

PUBLISHED PAPER

J. G. Martins, **A. C. de Oliveira**, P. S. Garcia, M. J. Kipper, **A. F. Martins**. Durable pectin/chitosan membranes with self-assembling, water resistance and enhanced mechanical properties. **Carbohydrate Polymers**, v. 188, pp. 136-142, **2018**. Impact Factor: **5.158.**

SUBMITTED MANUSCRIPT

A. C. de Oliveira, B. H. Vilsinski, E. G. Bonafé, J. P. Monteiro, M. J. Kipper, **A. F. Martins**. Chitosan content modulates durability and structural homogeneity of chitosan-gellan gum assemblies. **International Journal of Biological Macromolecules**, Submitted for Publication.

A. C. de Oliveira, R. M. Sabino, E. C. Muniz, K. C. Popat, M. J. Kipper, **A. F. Martins**. Chitosan/gellan gum ratio content is modulated to enhance the scaffolding capacity of polyelectrolyte assemblies. **Materials Science & Engineering C**, Submitted for Publication.

PATENT DEPOSIT

A. C. de Oliveira, B. H. Vilsinski, B. Medina, **A. F. Martins.** Processo para a fabricação de hidrogéis de quitosana e goma gelana e aplicações potenciais **(**Número de Registro: BR10201801432**)**, **2018**.

SUMMARY

CHAPTER 1: REVISION FROM THE LITERATURE

1.1. INTRODUCTION

Hydrogels are polymeric matrices which have potential applications in tissue engineering, agriculture, medicine, and pharmacy fields due to their high capacities to absorb water and biological fluids **(AHMED, 2015; CALÓ; KHUTORYANSKIY, 2015; HOFFMAN, 2002; SHUKLA et al., 2016)**. However, to be applied, hydrogels must be stable in aqueous systems, i.e., they must maintain their structures when used, and depending on the purposes, they often must have low degradation rate in the body **(Martins et al., 2018a, 2018b)**. Aiming technological applications, physical hydrogels can be prepared without the use of toxic crosslinking agents and following straightforward production methods **(FACCHI et al., 2018a)**.

Physical gellan gum-based hydrogels are prepared from aqueous systems at the presence of H_3O^+ or metallic cations. Vilela et al. produced physical microgels of CS/GG by ionotropic gelation using Ca^{2+} or K^+ ions as crosslinking agents **(VILELA et al., 2015)**. These cations can stabilize the anionic gellan gum (GG) polysaccharide chains by coulombic interactions, promoting formation of physical hydrogels. However, depending on some conditions of preparation, these GG-based hydrogels may quickly exhibit degradation rates and fast dissolution in water and biological fluids, necessitating an additional crosslinking step **(OSMAŁEK; FROELICH; TASAREK, 2014)**. The additional crosslinking step is required to impart stability and durability to the hydrogel. The H_3O^+ and metallic cations used as physical crosslinking agents of GG chains may increase the cytotoxicity of hydrogels, especially when they are degraded and dissolved **(MARTINS et al., 2015)**. However, the degree of cytotoxicity depends on the concentration of the cations used for preparing the hydrogels. Bonifacio et al. (2018), produced stable and cytocompatible GG/manuka honey-based hydrogels **(BONIFACIO et al., 2018a)**. These hydrogels were crosslinked with Ca^{2+} cations at 0.025% wt.%/vol.% and Mg^{2+} 0.50 wt.%vol.% in their respective physiological concentrations **(BONIFACIO et al., 2018a)**. Manuka honey improved the physicochemical and biological properties of the hydrogels, allowing better mechanical properties (Young's modulus between 102 to 143 kPa

depending on the composition of the material) and antimicrobial activity against *Staphylococcus aureus* and *Staphylococcus epidermidis.*

Chemical crosslinking agents are often used to provide more stable hydrogels, avoiding the water dissolution process **(GUILHERME et al., 2015)**. Common chemical cross-linking agents (epichlorohydrin, glutaraldehyde, and others) may induce cytotoxicity to the hydrogels, as well as decrease the biodegradability of the materials. These effects can reduce the biomedical potential of these materials, especially in the tissue engineering field **(COUTINHO et al., 2012)**. Physical hydrogels (commonly called polyelectrolyte complexes, PECs) are formed by mixing polymer solutions, involving polyelectrolytes of opposite charges **(PICONE; CUNHA, 2013; TENTOR et al., 2017)**. The coulombic and intermolecular interactions between polymer chains play an important role in the formation of PECs. Depending on the intensity of these interactions, PECs can be stable and irreversible **(MARTINS et al., 2015)**. PECs need to be cytocompatible to be applied as bandages (to promote wound healing), as scaffolds in tissue engineering arena and as drug carrier matrices in pharmaceutical purposes **(FACCHI et al., 2017a)**. At physiological pH, GG-based physical hydrogels crosslinked with metallic ions can be rapidly dissolved, while chemically crosslinked GG-based hydrogels are not biodegradable **(OSMAŁEK; FROELICH; TASAREK, 2014)**.

To overcome these complications, we can associate GG with chitosan (CS), aiming to create durable and cytocompatible PECs with low degradation rate in the physiological environment. CS is a cationic polysaccharide, soluble at dilute acid solutions **(RINAUDO, 2006)**. Here, CS will replace the conventional and metallic crosslinking agents used to produce physical GG hydrogels. Depending on the developed methodology, CS/GG PECs can occur without typical precipitation of oppositely charged polyelectrolytes in solution **(MARTINS et al., 2018a, 2018c)**. The formation of PECs by precipitating of polyelectrolytes in solution is a straightforward way to obtain physical hydrogels **(MARTINS et al., 2015)**. However, the precipitation process often promotes formation of PECs with heterogeneous and brittle structures **(FACCHI et al., 2017a)**. Aiming development of scaffold-based materials, these properties must be avoided because PECs must have structural homogeneity with interconnected pores networks to mimic the extracellular membrane matrix (ECM) functions and, then act as scaffold devices **(BOMBALDI DE SOUZA et al., 2018)**.

Kumar et al. prepared CS/GG nanoparticles by precipitating, using CS/GG systems with total polymer concentrations ranging from 0.01 to 0.05% wt.%/vol.% **(KUMAR et al., 2016)**. A current review paper based on GG blends, addressed a brief section on the production of CS/GG PECs and their potential applications **(ZIA et al., 2018)**. In general, these PECs are prepared from the precipitation of oppositely charged polyelectrolytes in aqueous solution, i.e., anionic GG and cationic CS can mainly be assembled by electrostatic interactions of their ionized $-COO^-$ and $-NH_3^+$ groups to form PECs **(AMIN; PANHUIS, 2011)**.

Therefore, this work has proposed a new and straightforward method to create durable, and cytocompatible CS/GG hydrogel scaffolds without chemical and metallic crosslinking agents. PECs were formed using different CS/GG weight ratios (wt.%/wt.%), blending CS and GG solutions at 60°C. It was demonstrated the production of thermosensitive PECs (avoiding precipitation) with homogeneous structures, high porosities and low degradation rates in phosphate buffer solution (PBS, pH 7.4) and simulated gastric fluid (SGF, pH 1.2). These properties are essential for the development of scaffolds **(AMIN; PANHUIS, 2011)** The sol-gel transition temperatures and the times required to achieve the gelation of the samples were also evaluated. Assays of cytotoxicity, cell adhesion, and proliferation were investigated, as well.

1.2. HYDROGELS

Hydrogels are three-dimensional polymer networks composed of hydrophilic moieties **(FERNÁNDEZ-FERREIRO et al., 2015; WANG; WEN; BAI, 2016)**. Hydrogels have great capacities to absorb biological fluids and water, resembling living tissues, and they can maintain their three-dimensional structures when applied **(AHMED, 2015; CALÓ; KHUTORYANSKIY, 2015; SHUKLA et al., 2016)**. Polysaccharide-based hydrogels may exhibit cytocompatibility, biodegradability, and response to the changes in external stimuli, such as alterations in temperature, ionic strength, and pH **(KAMOUN; KENAWY; CHEN, 2017)**. These traits have made hydrogels interesting for technological applications, mainly in medicine, pharmacy and tissue engineering fields.

Hydrogels can be classified in chemical and physical-based materials. Chemical hydrogels are formed by the establishment of covalent bonds between polymer networks and crosslinking agents. Fig. 1A depicts the chemical structure of poly(vinyl alcohol)-based hydrogel crosslinked with glutaraldehyde, following a chemical process **(MORE et al., 2010)**. Overall, chemical hydrogels have organized and irreversible structures. This dissertation will focus on physical hydrogels, commonly called as PECs **(BERGER et al., 2004).** These materials are reversible; however, this property is related to the association degree between the polymer chains **(Martins et al., 2018b, 2018a)**. In this case, physical hydrogels are formed by the establishment of secondary-order forces (intermolecular interactions) and first-order interactions (electrostatic interactions) between polymer chain segments (Fig. 1B) **(INSUA; WILKINSON; FERNANDEZ-TRILLO, 2016)**. Recently, our research group has received attention because we published three papers about durable and irreversible PECs **(FACCHI et al., 2017b; MARTINS et al., 2018a, 2018b).** These PECs were applied as scaffold devices on adipose stem cells **(MARTINS et al., 2018a)** and adsorbent materials to treat wastewater **(FACCHI et al., 2017b).**

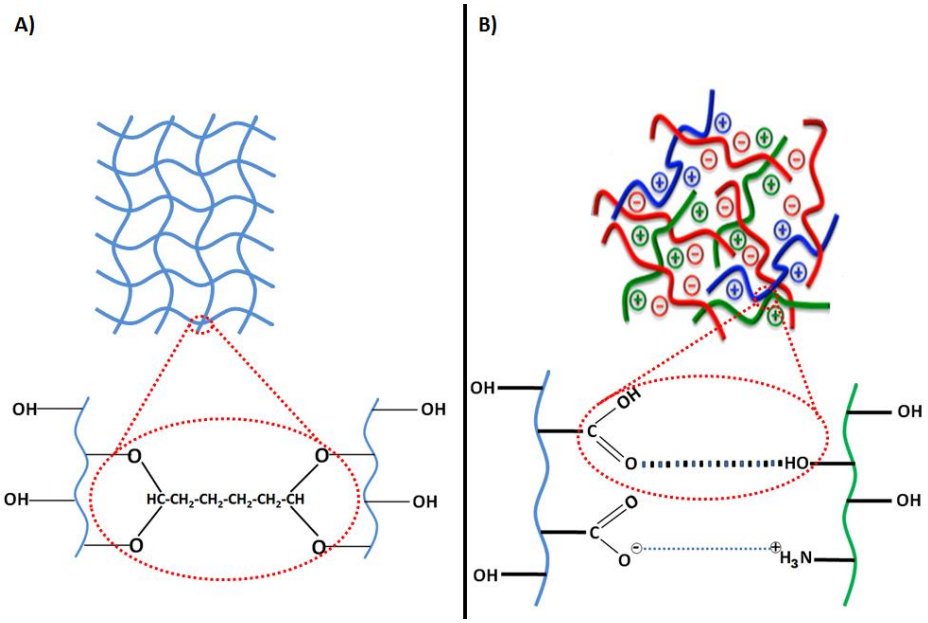

Figure 1. Hypothetical structures of the hydrogels: chemical (A) and physical (B).

Hydrogels can act as drug carrier matrices and as scaffolds to promote regeneration and repair of organs and tissues **(SAUL; WILLIAMS, 2013)**. In agriculture, they can act as soil conditioners and devices to delivery fertilizers to the soils **(GUILHERME et al., 2015)**. **TENTOR et al., (2017)** developed cytocompatible and thermosensitive pectin/CS scaffolds (PECs) associated with gold nanoparticles. These PECs promoted proliferation of mouse pre-osteoblastic cells (MC3T3-E1 cells). **NAAHIDI et al., (2017)** published a review paper depicting hydrogels based on natural (collagen, gelatin, pullulan, and hyaluronic acid) and synthetic polymers (poly(lactic acid), poly(glycolic acid), poly(ethylene oxide), poly(ethylene glycol), and poly(caprolactone)), and their applications as scaffolds onto cartilage, neural, skin, vocal cord, connective tissue, eye, facial, vascular, stem cell, and soft tissues. Also, superabsorbent hydrogels based on polysaccharides (pectin, gums, starch, gum alginate and others) have been used as soil conditioner agents and as nutrient carriers **(GUILHERME et al., 2015)**. Yet, hydrogels are used as adsorbent agents to treat effluents and wastewater, containing dyes and toxic metals **(HUANG et al., 2013; MOHAMED; ELELLA; SABAA, 2017)**. Thus, PECs formed by associating of CS and GG can have technological interests, mainly in biomedical field. This study will investigate this fact for the first time.

1.3. GELLAN GUM

GG is a linear, anionic and water-soluble polysaccharide of high molecular weight, composed of α-L-rhamnose, β-D-glucose and β-D-glucoronate units in the ratio 1:2:1, respectively **(OSMAŁEK; FROELICH; TASAREK, 2014)**. GG is an excellent stabilizing and emulsifying agent; then, it is widely used in the food industry **(PRAJAPATI et al., 2013)**. This polysaccharide was discovered in 1978, and since then, it has been commercialized by CP Kelco Company **(OSMAŁEK; FROELICH; TASAREK, 2014)**. GG is obtained through the extracellular secretion of the microorganism *Sphingomonas elodea*, throughout the aerobic fermentation process. In its native form, GG has a high acylation degree; however, the acyl groups can be removed by the alkaline hydrolysis **(AGNIHOTRI; JAWALKAR; AMINABHAVI, 2006; OSMAŁEK; FROELICH; TASAREK, 2014)**. Therefore, GG can be found in

two forms, one partially acetylated containing high acylation level (Fig. 2A) and another deacetylated of low acylation content (Fig. 2B) **(GIAVASIS; HARVEY; MCNEIL, 2008)**.

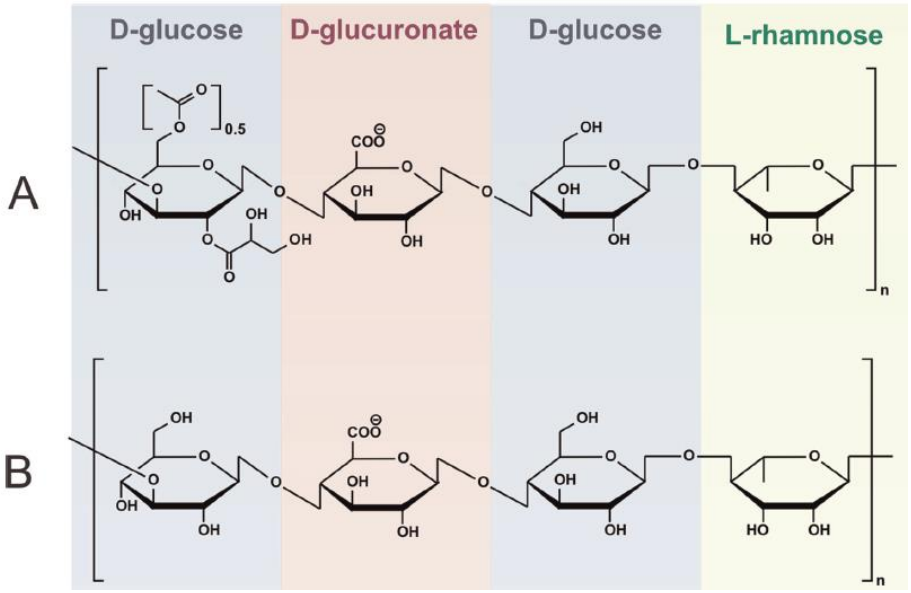

Figure 2. Chemical structures of the gellan gum: with high (A) and low acylation degree (B) **(OSMAŁEK; FROELICH; TASAREK, 2014)**.

Because of its size, ester groups can difficult the package of GG chains when aqueous GG solutions are combined with metallic cations. So, the ester sites may disturb the formation of physical GG hydrogels; however, GG chains with a high acylation degree are crosslinked at the presence of monovalent, divalent or trivalent cations **(AGNIHOTRI; JAWALKAR; AMINABHAVI, 2006)**. In this case, a metallic crosslinked GG-based hydrogel has flexibility and transparency, whereas GG of low acylation degree yields rigid and opaque hydrogels **(GIAVASIS; HARVEY; MCNEIL, 2008)**. GG can also be associated with cationic polysaccharides (such as CS) to create PECs by precipitation **(NUNES et al., 2017a; ZHANG et al., 2018)**.

In aqueous solution at temperature conditions ranging from 60 to 90°C, GG chains are ionized, allowing aleatory configurations (Fig. 3; left panel). In this way, the ionization of –COOH sites (pK_a 3.5) generates electrostatic repulsion between the GG chains, preventing the formation of double helices (even at the presence of cations), responsible for the gelation process **(Coronato, 2010)**. At low temperatures, the gelation of GG is favored by changing the ionic strength (presence of metallic cations), by altering of pH at range from 3.0 to 5.0, and by increasing GG

concentration. At low temperatures (for example at room temperature), the presence of cations imparts double helices on GG chains due to the stabilization of the ionized $–COO^-$ groups (Fig. 3; right panel) **(Coronato, 2010)**. Thus, when GG/cations mixtures are cooled, reversible double helix configurations take place, forming ordered states, and leading to the gelation of the GG chains (Fig. 3; right panels).

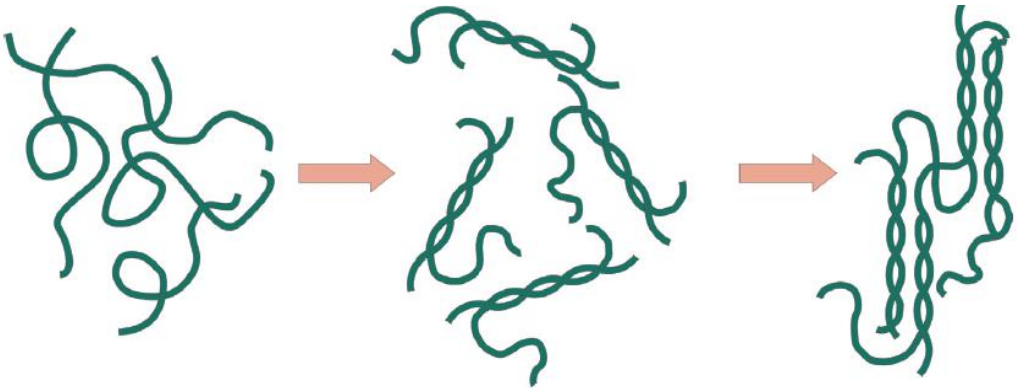

Figure 3. GG chains in aqueous solution at high temperature (range from 60 to 90ºC) conditions (left panel). Cooling process of GG chains in aqueous solutions containing metallic cations and establishment of double helix configurations (central panel); GG chains entirely crosslinked at low temperature (right panel) **(OSMAŁEK; FROELICH; TASAREK, 2014)**.

1.4. CHITOSAN

CS is a linear, cationic polysaccharide, composed of D-glucosamine and N-acetyl-D-glucosamine units, linked by β(1→4) glycosidic linkages **(AMIN; PANHUIS, 2011; VILELA et al., 2015)**. CS is mainly obtained from the alkaline deacetylation of chitin, which is the second most abundant polysaccharide in the planet **(LIU et al., 2014; PICONE; CUNHA, 2013)**. The CS is a cationic polysaccharide that has low solubility in water and is soluble in dilute acid solutions due to the protonation of $–NH_2$ groups in its structure **(TANG et al., 2012)**. Protonation disturbs the CS-CS intermolecular interactions and provides the establishment of ion-dipole interactions with water molecules, making CS soluble. This feature enables formation of CS-based PECs when CS-based solutions are combined with polyanionic

polysaccharide solutions, such as pectin, alginate, gums, glycosaminoglycans, and others **(RINAUDO, 2006)**.

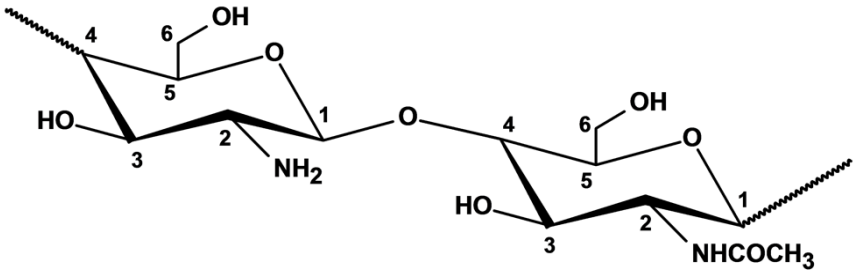

Figure 4. Chemical structure of the chitosan.

CS has renowned technological potential **(AZEVEDO et al., 2007)**. The hydrophilic moieties (–NH_2 and –OH at C2, C3 and C6 positions, respectively; Fig. 4) can bind to the toxic metals and dyes to remediate contaminated aqueous systems **(MOURA et al., 2007)**. Moreover, CS exhibits properties of cytocompatibility, biodegradability, mucoadhesivity, antimicrobial activity, and others **(AMIN; PANHUIS, 2011; FACCHI et al., 2016; HAJJI et al., 2016)**. Due to these excellent traits, CS and CS-based materials (hydrogels) are being used in several industrial sectors. CS-based materials have been applied in agriculture **(GUILHERME et al., 2015)**, as adsorbents and coagulants materials for environmental purposes **(ZEMMOURI et al., 2012)**, as films in food industry **(BORDERÍAS; SÁNCHEZ-ALONSO; PÉREZ-MATEOS, 2005)**, materials for cosmetic industries (products based on exfoliating and moisturizing creams and toothpaste) **(TAVARIA et al., 2013)**, and as devices for medical-pharmaceutical arena (supports for dental implants, contact lenses, systems to promote bone reconstitution and drug carrier matrices) **(AZEVEDO et al., 2007; RINAUDO, 2006)**.

1.5. SCAFFOLDS

Polysaccharide-based scaffolds can play an important role in biomedical applications because they have similar structures to the ECM (porosity in interconnected pore networks, hydrophilicity-hydrophobicity balance, cytocompatibility, and others) **(AMIN; PANHUIS, 2011; LIU et al., 2013)**. The ECM

must mediate the cellular interactions with their environment **(FACCHI et al., 2017a).** The ECM provides mechanical support for cell attachment, and signals that control cell proliferation, cell orientation, and maintenance of cell differentiation **(FACCHI et al., 2017a)**. The ECM thereby modulates so-called “cell fate decisions.” Overall, ECM components are the fibrillar and adhesive proteins, glycosaminoglycans, and proteoglycans **(HEDAYATI et al., 2018)**. Proteoglycans are chemical structures composed of glycosaminoglycans covalently bound to proteins **(HEDAYATI et al., 2018)**.

Therefore, scaffolds used for tissue engineering purposes should similarly promote cell adhesion and provide mechanical and chemical cues that can guide cell shape, cell migration, and other important cellular activities. Therefore, we envision developing CS/GG PEC scaffolds for tissue engineering purposes. These PECs will be created following a new methodology, avoiding precipitation of polyelectrolytes in aqueous solution. We will report suitable CS/GG weight ratios for obtaining PEC scaffolds with high stability, cytocompatibility, and ability to support bone stem cell culture.

LIU et al., (2013) associated CS-based fibers with GG hydrogels, in which improvement in their properties, as a storage modulus, which is 4.6 times higher between hydrogel from chitosan fibers and gellan gum when compared to gellan hydrogel only was observed. Through this improvement, these hydrogels have potential to be used as scaffolds, thus obtaining the stability required for such application. **(LIU et al., 2013)**. MARTINS et al., (2018a) prepared pectin and chitosan (Pec/CS) PEC membranes. These membranes promoted adhesion, growth, and proliferation of stem cells derived from human adipose tissue **(MARTINS et al., 2018a)**. GANTAR et al., (2014), developed gellan gum hydrogels reinforced with bioactive nanoparticle glass (GG-BAG) for application in bone tissue engineering. The authors noted that after the addition of BAG, the hydrogel obtained more homogeneous pores and Young's modulus was between 1.9 and 1.2 MPa, in the dry form and in the hydrogel form, consequently. These results are superior to those found with the GG-only hydrogel. This improvement enables the application of this hydrogel as scaffold, making it promising to adhere, grow and proliferate the adipose stem cells **(GANTAR et al., 2014)**. ZHU et al., (2009), obtained collagen-chitosan composites and used them as scaffolds for the proliferation of human adipose tissue-

derived stem cells (ADSC). The authors have achieved with this polymer, porosity, bibulous capacity, biodegradation and cytocompatibility with ADSCs, thus having adhesion, proliferation, and differentiation of these cells **(ZHU et al., 2009).**

CHAPTER 2: CHITOSAN CONTENT MODULATES DURABILITY AND STRUCTURAL HOMOGENEITY OF CHITOSAN-GELLAN GUM ASSEMBLIES

Abstract

Here we report a new and straightforward method to yield durable polyelectrolyte complexes (hydrogel PECs) from gellan gum (GG) and chitosan (CS) assemblies, without metallic and covalent crosslinking agents, commonly used to produce GG and CS-based hydrogels, respectively. This new approach overcomes challenges of obtaining stable and durable GG-based hydrogels with structural homogeneity, avoiding precipitation and aqueous instability, typical of PEC-based materials. PECs are created by blending CS:GG solutions (at 60°C) with GG:CS weight ratios between 80:20 to 40:60. X-ray photoelectron spectroscopy (XPS) analysis shows that CS-GG chains are interacting by electrostatic and intermolecular forces, conferring a high degree of association to the neutralized PECs, characteristic of self-assembling of polymer chains. The CS:GG weight ratio can be tuned to improve polyelectrolyte complex (PEC) high porosity, stability, porous homogeneity, and degradation rate. Physical and thermosensitive CS/GG-based hydrogels can have advantages over conventional materials produced by chemical processes.

Keywords: Polyelectrolyte Complex, Hydrogel, Self-assembling, Durability

2.1. INTRODUCTION

Physical and thermosensitive GG-based hydrogels can be created by addition of metal cations (potassium, calcium, aluminum, and others), and cooling of the GG-cation solutions **(PRAJAPATI et al., 2013)**. At lower temperatures, the polymer conformation of GG is altered because of a coil-to-double helix transition.

669 Monovalent or polyvalent cations can stabilize this conformation by electrostatic
670 interactions **(SALUNKE; PATIL, 2016)**. In the absence of these cations,
671 deacetylated GG-based hydrogels are also created by the reduction of pH **(DE**
672 **SOUZA et al., 2016)**.

673 Chemical crosslinking agents are also used to provide water-stable
674 polysaccharide-based hydrogels **(GUILHERME et al., 2015)**. As an alternative to
675 chemical and ionic crosslinking, physical hydrogels, commonly referred to as PECs,
676 are created by the establishment of physical interactions (electrostatic and
677 intermolecular interactions), usually between polycation-polyanion polymer pairs in
678 aqueous solutions **(MARTINS et al., 2015)**. Aiming toward applications in the
679 biomedical, pharmacy, food industry, agriculture, environmental, and other fields,
680 hydrogels need to be stable at physiological pH with low degradation rates to
681 maintain their structures and in many cases, their three-dimensional porous
682 structures **(FACCHI et al., 2017a)**. Therefore, we are intending to create durable GG
683 hydrogels, by associating anionic GG with CS, avoiding conventional crosslinking
684 agents (metallic cations, glutaraldehyde, epichlorohydrin, genipin, and others) to
685 produce polysaccharide-based hydrogels. CS is a well-known cationic
686 polysaccharide with aqueous solubility in dilute acid solutions and because of this, it
687 has been chosen to yield PECs by associating with polyanionic polymers **(FACCHI et**
688 **al., 2017b)**.

689 Here, we are proposing a new method to create physical and stable
690 hydrogels based on CS/GG assemblies, avoiding typical precipitation of PEC-based
691 materials and their aqueous instability. According to a review paper, physical CS/GG
692 PECs have not received significant attention yet **(LUO; WANG, 2014)**. Another
693 current review paper based on GG blend studies related a brief section concerning
694 the production of CS/GG PECs and their applications **(ZIA et al., 2018)**. Overall,
695 these PECs have been prepared from precipitation of oppositely charged
696 polyelectrolytes in aqueous solution.

697 This study has proposed a way to create stable CS/GG PECs free of
698 precipitation. PECs are produced from different CS:GG weight ratios, blending
699 CS/GG solutions at 60°C. We demonstrate production of stable PECs with
700 thermosensitivity, porosity, water stability, self-assembling, structural homogeneity,

and slow degradation behavior in phosphate buffer solution (PBS, pH 7.4) and simulated gastric fluid (SGF, pH 1.2). These properties are achieved over a range of CS:GG weight ratio in the final blend composition. The physicochemical properties of these materials, including sol-gel temperature and gelation time are also reported here.

2.2. MATERIALS AND METHODS

2.2.1. Materials

KELCOGEL® gellan gum (an anionic exopolysaccharide) of low acyl degree and molar weight between 2.0 to 3.0×10^5 g mol^{-1} **(PRAJAPATI et al., 2013)**. was graciously donated by CP Kelco Co., Limeira-SP, Brazil. Chitosan (CS) with deacetylation degree equal to 85% and average molar weight of 87×10^3 g mol^{-1} was purchased from Golden-Shell Biochemical (China) **(FACCHI et al., 2018b)**.

2.2.2. Hydrogel preparation

Aqueous solutions of CS and GG (1.0 wt.%/vol.%) were individually prepared by dissolving the polysaccharides at 60°C for 10 min. CS solution was prepared in dilute aqueous HCl solution (pH≈1.0), while GG solution was prepared in deionized water (pH≈6.0). CS/GG hydrogels were created in different CS:GG weight ratios (at a whole polymer content of 1.0 mg mL^{-1}), by blending CS and GG solution aliquots from their previously established solutions (Table 1). For obtaining PECs, aliquots of the GG-solution (1.0 wt.%/vol.% at 60°C) are slowly dropped into suitable aliquots of the CS-solution (1.0 wt.%/vol.% at 60°C) (Table 1). After dropping, the system is maintained under magnetic stirring for 5.0 min, to form homogeneous CS/GG solutions (Fig. 1). Then, flasks (10 mL) containing CS/GG blends (6.0 mL) were conditioned in a water bath at 25°C for 2.0 h to promote the physical crosslinking (Fig. 1). Thermosensitive hydrogels were removed from the flasks and soaked in 50 mL deionized water under gentle magnetic stirring. An aqueous NaOH solution (0.010 mol L^{-1}) was slowly dropped into the system to raise the pH to at least 5.8. After neutralization, all samples were frozen and lyophilized (-50°C for 72 h). Also, after production and before neutralization, the as-obtained PECs were frozen and lyophilized to yield unneutralized hydrogels.

Table 1. Experimental conditions used to create CS/GG PECs and results of acquisition, and disintegration during neutralization step.

Samples	CS (mL:g)	GG (mL:g)	CS:GG weight ratio	Acquisition	Disintegration[a]
CS/GG(90-10)	5.4:0.054	0.6:0.006	90:10	No	-
CS/GG(80-20)	4.8:0.048	1.2:0.012	80:20	Yes	No
CS/GG(70-30)	4.2:0.042	1.8:0.018	70:30	Yes	No
CS/GG(60-40)	3.6:0.036	2.4:0.024	60:40	Yes	No
CS/GG(50-50)	3.0:0.030	3.0:0.030	50:50	Yes	No
CS/GG(40-60)	2.4:0.024	3.6:0.036	40:60	Yes	Yes
CS/GG(35-65)	2.1:0.021	3.9:0.039	35:65	No	-

[a]Samples that disintegrated but did not dissolve during the neutralization step. The hydrogel is obtained but without a regular structure.

2.2.3. Final CS:GG ratios in the hydrogel compositions

The same procedure adopted by Martins et al. **(MARTINS et al., 2018b)** was used to determine the yield of complexation between CS and GG. Supernatants (≈50 mL) obtained during the neutralization/washing step were kept in an ultrasound bath for 10 min (25°C) to disperse remaining CS/GG PEC particles and uncomplexed polymers released throughout the washing. Supernatant aliquots (15 mL) were removed, frozen and lyophilized (-50°C for 48 h). The mass of the solid material, comprising both GG and CS was measured from the lyophilized supernatants. The yield of complexation (%) was identified by difference from the lyophilized mass of solid compared to the whole polymer weight (0.30 g) used to create PECs in Table 1. For each composition, this measurement was performed in duplicate.

2.2.4. Hydrogel properties

2.2.4.1. Thermosensitive

The sol-gel temperatures and necessary times to achieve the gel state were determined by tilting method **(TENTOR et al., 2017)**. This approach was chosen because the CS/GG hydrogels do not present thermal reversibility. The tilt method involves tilting flasks containing CS/GG solution; the temperature at which the CS/GG solution no longer flows is taken as the gelation temperature. Sealed flasks of 10 mL containing CS/GG-solutions (6.0 mL at 60°C) previously reported in Section 2.2.3 were put into a glass reactor coupled to a thermostated bath at 60°C. The

temperature of the reactor was measured by a digital thermometer (model ITTH-1400). The bath temperature was adjusted to 58°C, and then continuously reduced at a rate of 2°C every 30 min, until gelation was reached. It is estimated that the gel state is the temperature at which each CS/GG suspension no longer flows after tilting the vial (tilting method). Also, the necessary time to achieve the gel point is assessed, soaking flasks containing CS/GG blends (6.0 mL) at 60°C in a water bath at 25°C. The time at which CS/GG solution no longer flow is taken as the gelation time. These processes were repeated twice (n=2).

2.2.4.2. In vitro degradation test

After washing, wet and neutralized PECs (at equilibrium state) were weighed (samples of approximately 15×10 mm) to determine their wet weights (W_{wet-I}). The wet hydrogels were soaked in 50 mL of PBS (pH = 7.4) or SGF (pH = 1.2) and incubated at 37°C with shaking (100 rpm) **(CHEN et al., 2010)**. At desired time intervals, the samples were removed from the solutions and weighed to measure the final wet weight (W_{Wet-F}). The degradation/dissolution (%) was assessed using the following Equation

$$Degradation\ (\%) = \frac{(W_{Wet-I} - W_{Wet-F})}{W_{Wet-I}} \times 100 \qquad (1)$$

2.2.5. Characterization

Surface chemistry of the hydrogels was evaluated using a Phi Electronics 5800 Spectrometer (Chanhassen, MN) **(ROMERO et al., 2015)**. The X-ray photoelectron spectroscopy (XPS) was performed with a monochromatic Al Kα X-ray source (hν = 1486.6 eV), a hemispherical analyzer, and a multichannel detector. High-resolution spectra were obtained using a 23.5 eV analyzer pass energy with 0.10 eV steps and an X-ray spot of 800 μm. All spectra were obtained with a photoelectron take-off angle of 45°. A low-energy electron gun was used for charge neutralization. Spectra curve fitting was done using Origin version 8.5. Curve fitting of all spectra used a Shirley background. Gaussian peaks were fit according to expected functional groups. The height of each peak was fit first while keeping each

784 peaks' position, full-width half max (fwhm) and percent Gaussian fixed. Then the
785 fwhm, percent Gaussian, and finally position was fit while minimizing the chi-squared
786 value. The content (%) of C1s, O1s, and N1s was statistically analyzed using ANOVA
787 and Tukey tests at a 5% significance level (using the program GraphPad Prism 6.0),
788 using duplicate XPS spectra (survey) for each sample. This analysis was carried out
789 at Colorado State University (CSU), USA.

790 TGA/DTG analyses were carried out in a thermogravimetric analyzer
791 (Shimadzu, model TGA50, Japan) at a 10°C min^{-1} rate, from 25°C to 650°C, under
792 50 mL min^{-1} argon purge. DSC analyses were performed on a calorimeter
793 (Shimadzu, model DSC60 Plus, Japan) operating at the following conditions: heating
794 rate of 10°C mim^{-1}, from 20°C to 290°C, under 50 mL min^{-1} nitrogen purge.

795 The morphology of the hydrogels was investigated through SEM. The
796 samples were sputter-coated with palladium-gold alloy (Polaron SC 7620 Sputter
797 Coater, Quorum Technologies, Newhaven, UK) at a thickness of 20 nm (10-15 mA,
798 under a vacuum of 130 mTorr). The SEM (JSM-6500F, field emission scanning
799 electron microscope, JEOL, Japan) was operated at an accelerating voltage of 10
800 kV, and three to six locations on each sample were imaged. This analysis was
801 carried out at Colorado State University (CSU), USA.

802 2.2.6. Statistical analysis

803 The results were statistically analyzed by ANOVA and Tukey tests at a 5%
804 significance level (GraphPad Prism 6.0).

805 2.3. RESULTS

806 2.3.1. Thermosensitivity and yield of complexation

807 CS/GG blends (60°C) were obtained by blending CS solutions (prepared in a
808 dilute 0.10 mol L^{-1} HCl aqueous solution at 60°C) with GG solutions (prepared in
809 deionized water at 60°C). When prepared under these conditions, CS/GG blends are
810 homogenous, and hydrogel PECs are acquired after cooling of CS/GG solutions (Fig.
811 5). GG chain segments can stabilize charged CS macromolecules, establishing
812 electrostatic interactions between $-COO^-$ and $-NH_3^+$ sites on GG and CS networks,

respectively. Furthermore, the acid condition in the CS-solution (pH 1.0) can also further stabilize the GG double helix conformation **(DE SOUZA et al., 2016)**, imparting a high degree of intramolecular association between polymer backbones.

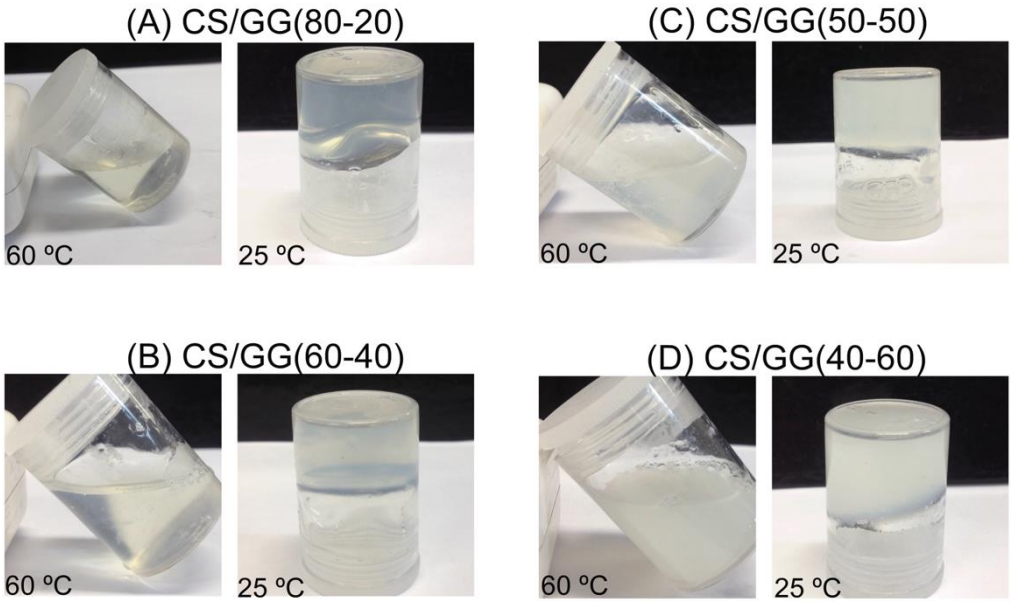

Figure 5. Digital images of the CS/GG blends at 60□C and CS/GG PECs at 25□C (unneutralized samples).

Increasing GG content in the blend results in more opaque hydrogels (Fig. 1D). Hydrogels are obtained at compositions ranging from 80:20 to 40:60 (CS:GG). PECs are not formed at 90:10 CS:GG weight ratio because of the low GG concentration and few negative charges. Similarly, at the 35:65 CS:GG weight ratio the GG excess increases the negative charge density in the blend. To better understand these composition limits, XPS analysis yielding information about the ammonium/carboxylate ratios was performed. GG-solutions were prepared at pH 6.0 (deionized water), resulting in complete ionization of the GG macromolecules (pK_a 3.5) **(OSMAŁEK; FROELICH; TASAREK, 2014)**. Therefore, mixing CS and GG solutions at 80:20 to 40:60 CS:GG weight ratio range led to the formation of stable PECs (Fig. 5). To our knowledge, this is the first report of CS/GG hydrogel PECs prepared by combining CS and GG solutions, without precipitation and addition of exogenous cross-linking chemistries or metal ions.

The sol-gel temperature, as well as the time to achieve the sol-gel phase transition, were determined using the tilting method (Table 2). According to the

834 literature, temperatures of sol-gel phase transition assessed from the tilting method
835 are in good agreement (within 1.0°C) with those provided by a more accurate
836 rheological apparatus **(TENTOR et al., 2017)**. After gelation, all CS/GG hydrogels did
837 not display thermo-reversibility behavior, i.e., CS/GG blend solutions were not
838 obtained upon soaking flasks containing CS/GG PECs in a water bath at 60°C. This
839 indicates a very high thermal stability of the hydrogels. The temperature of sol-gel
840 transition occurs in the 48-52°C range and gelation time is between 1.3-1.5 minutes
841 (Table 2).

842 **Table 2.** Properties of the hydrogel PECs: necessary temperature and time to achieve the sol-gel
843 phase transition and yield of complexation.

Samples	Sol-gel temperature (°C)	Time (min)	Yield (%)
CS/GG(80-20)	48±1	1.4±0.1	98±1
CS/GG(70-30)	51±1	1.5±0.1	99±1
CS/GG(60-40)	48±1	1.4±0.1	100±1
CS/GG(50-50)	49±1	1.3±0.1	99±1
CS/GG(40-60)	52±1	1.4±0.1	99±1

844

845 For all of the compositions that formed gels, the gelation temperature and
846 gelation time are not strong functions of the composition. All of these compositions
847 achieve association between CS and GG macromolecules. The acidic condition of
848 the CS-solution promotes stability of the GG double helices, imparting stability to the
849 gel state, and resulting in high gelation temperatures and low times to reach the sol-
850 gel phase transition compared to other reports of GG-based hydrogels. The sol-gel
851 temperature transition of GG-based hydrogels crosslinked by metallic cations
852 mainly depends on the concentration and valency of the crosslinking agent. Divalent
853 cations impart higher stability to GG-based hydrogels than monovalent cations
854 **(KIRCHMAJER et al., 2014)**.

855 The sol-gel phase transition of a GG-Na^+-based hydrogel crosslinked by Na^+
856 ions at 100 mmol L^{-1} was achieved at 46°C. GG-Ca^{2+} hydrogel crosslinked with 5.0
857 mmol L^{-1} Ca^{2+} solution displayed so-gel phase transition at 37°C, whereas a GG

hydrogel free of metallic crosslinking agents exhibited sol-gel phase transition at 30°C **(KIRCHMAJER et al., 2014)**. GG/poloxamer hydrogels were formed in physiological medium **(DEWAN et al., 2017)**. The temperature of sol-gel transition (determined by tilt method) of the GG/poloxamer hydrogels occurred at 25-32°C range, and depended on the GG:poloxamer blend composition **(KIRCHMAJER et al., 2014)**. Here, CS/GG hydrogels were imparted with greater thermal stability, and they were produced at high complexation yields (98-100%) (Table 2). These properties were achieved due to the strong association between CS and GG polymer chains. These properties are not found in conventional physical GG-based hydrogels.

2.3.2. In vitro degradation

The stability of the neutralized and wet hydrogels was determined in PBS and simulated gastric fluid (SGF) for 1, 3, 5, 7 and 14 days at 37°C (Fig. 6). The hydrogel PECs are more stable against degradation in PBS buffer than in SGF. Degradation rates also depend on the CS:GG weight ratio used to create PECs. The CS/GG(60-40) hydrogel had the highest stability in both evaluated media. After 14 days, CS/GG(60-40) hydrogel shows degradation of only 12% in PBS and 26% in SGF (Fig. 6). The 60:40 CS:GG condition is the best to promote a stable hydrogel because CS and GG networks should efficiently interact, imparting strong association between their chains.

Hydrogels created from the 80:20 and 50:50 CS:GG weight ratios (samples CS/GG(80-20) and CS/GG(50-50)) do not exhibit high water stability. In PBS, the CS/GG(80-20) exhibited weight losses of 25% and 40% after 5 and 14 days, respectively (Fig. 6). At the same experimental conditions, CS/GG(50-50) hydrogel had weight losses of 2% and 43% after 5 days and 14 days, respectively. In SGF, CS/GG(80-20) PEC degraded 33% after 5 days and 75% after 14 days, whereas in the same period, CS/GG(50-50) hydrogel degraded approximately 24% between 5 days and 14 days of study.

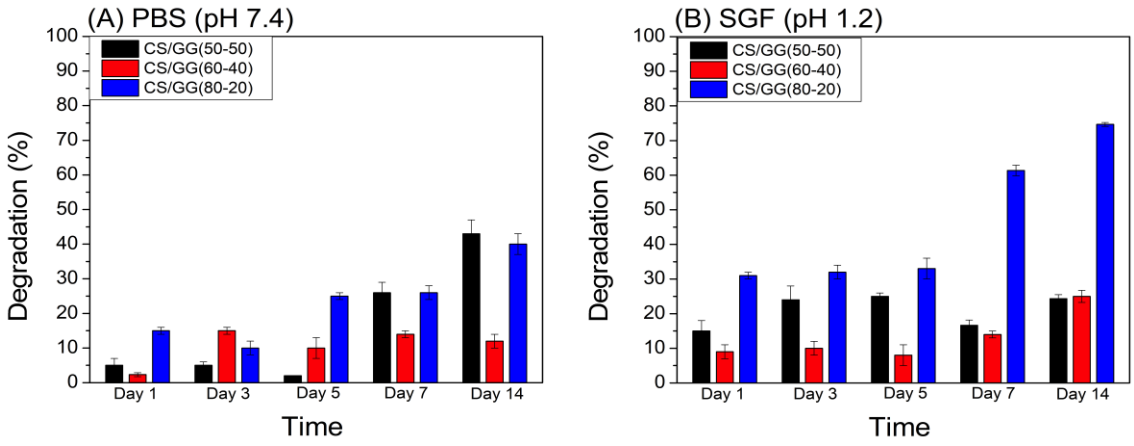

885

886 **Figure 6.** Results of degradation determined in PBS and SGF media at 37°C.

887

888 In SGF (pH 1.2), the CS/GG(80-20) hydrogel containing a CS excess has
889 lower stability because CS macromolecules are protonated, imparting solubility and
890 consequently hydrogel degradation/dissolution. All hydrogel samples were
891 neutralized to at least pH 5.8 prior to the degradation experiments. Increasing the pH
892 from 5.8 (neutralized PECs) to 7.4 (PBS) decreases the degradation rate likely
893 because CS has a reduced charge density ($pK_a \approx 6.5$) as the pH is increased from pH
894 5.8 to 7.4 and becomes insoluble. However, for hydrogels with increased GG content
895 (50:50), the increased negative charge density in the hydrogel matrices imparts low
896 water stability. This explains the lower stability of the CS/GG(50-50) hydrogel in PBS
897 after 14 days (Fig. 6A). Also, during neutralization, the CS/GG(40-60) hydrogel can
898 lose its structure (without dissolving, Table 1) due to the slow pH alteration, and the
899 consequent rise of negative charge density on GG chains. Considering the
900 degradation assays performed with the wet hydrogels, CS/GG assembly should be
901 yielded at 60:40 CS:GG weight ratio to minimize the weight loss during the
902 degradation test **(FACCHI et al., 2017a)**.

903 On the other hand, comparing these results with degradation findings for
904 other physical GG-based hydrogels, CS/GG PECs display high water stability.
905 Concentrated aqueous GG-solution (2.0 wt.%) provided a hydrogel in PBS buffer
906 with degradation percentage of 30% after only 4 h **(YU; KAONIS; CHEN, 2017)**. A
907 hydrogel-based on GG/poloxamer prepared at 0.30 wt.% GG and 18 wt.% poloxamer
908 content showed fast degradation, reaching 47% in an artificial tear fluid after only 7 h

(DEWAN et al., 2017). These other GG-based hydrogels exhibit much lower water stability than the hydrogels reported here. Consequently, researchers have proposed an additional chemical crosslinking of GG chains to stabilize the hydrogel structures to make them suitable for long-term biological applications **(FACCHI et al., 2017a; OSMAŁEK; FROELICH; TASAREK, 2014)**.

Physical CS-based hydrogels can also exhibit water stability depending on the adopted experimental procedure. CS-pectin PEC membranes prepared in an aqueous 0.10 mol L^{-1} HCl also presented high water stability during 14 days in PBS **(MARTINS et al., 2018b)**. Here, we present physical and stable CS/GG hydrogels prepared without chemical crosslinking, using a straightforward experimental procedure, and avoiding aqueous instability of oppositely charged polyelectrolyte mixtures.

2.3.3. Characterization

2.3.3.1. X-ray photoelectron spectroscopy

XPS was used to analyze the chemical composition of cross-sections of the dried PECs, obtained by fracturing. The results are interpreted, considering that all neutralized hydrogel samples imparted homogeneous structures. The chemistry of the PEC cross-sections was characterized using survey and high-resolution XPS spectra (Figs. 7). All XPS spectra show presence of O1s (534 eV), N1s (401 eV) and C1s (287 eV) (Fig. 7). The atomic contents of O1s, N1s, and C1s are presented in Table 3. The occurrence of nitrogen in XPS spectra confirms CS in the PEC structures. The oxygen content was increased at lower CS:GG ratios because GG includes carboxylic acid sites in its structure. Of note is that the N1s peak is more intense in CS/GG(80-20) XPS spectrum, imparting N1s content of 2.7% (Table 3). The content (%) of C1s, O1s, and N1s in CS/GG(80-20) is significantly different ($p \leq 0.05$) compared to the other samples because of the highest CS:GG weight ratio (Table 3).

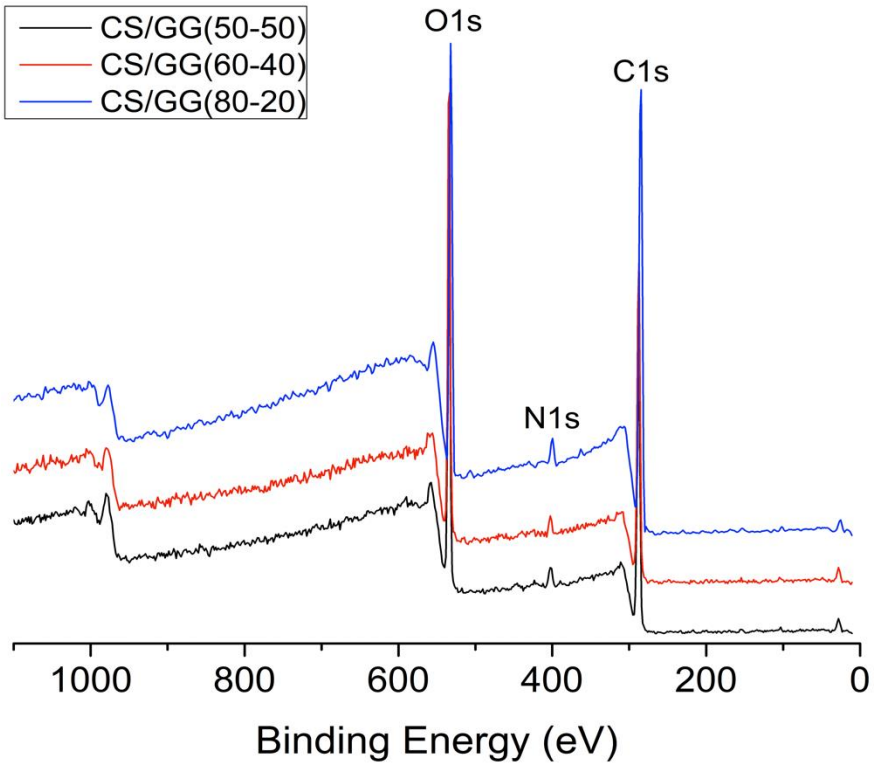

Figure 7. Survey XPS spectra of the neutralized PECs.

Table 3. Chemical composition of the hydrogels obtained from XPS analysis.

Samples	$-NH_3^+$ (%)[a]	$-COO^-$ (%)[b]	$-COO^-/-NH_3^+$	O1s(%)[c]	N1s(%)[c]	C1s(%)[c]
CS/GG(50-50)	74	4.3	3.1	40.0±0.2	1.9±0.3	62.1±0.1
CS/GG(60-40)	56	7.5	0.98	39.5±0.3	1.9±0.1	62.2±0.3
CS/GG(80-20)	37	5.8	1.0	28.7±0.4****	2.7±0.1*	68.6±0.5****

[a]Relative percentages of the NH_3^+ to total N determined from the peak areas in each high-resolution XPS spectrum for N1s.
[b]Relative percentages of the $-COO^-$ to total O determined from the peak areas in each high-resolution XPS spectrum for O1s.
[c]Comparing the same elements, the CS/GG(80-20) present a significant difference content (%) of O1s, N1s, and C1s concerning the other PECs (**** is indicating $p \leq 0.0001$ and * is indicating $p \leq 0.05$).

High-resolution XPS spectra for O1s and N1s envelopes are presented in Fig. 8.

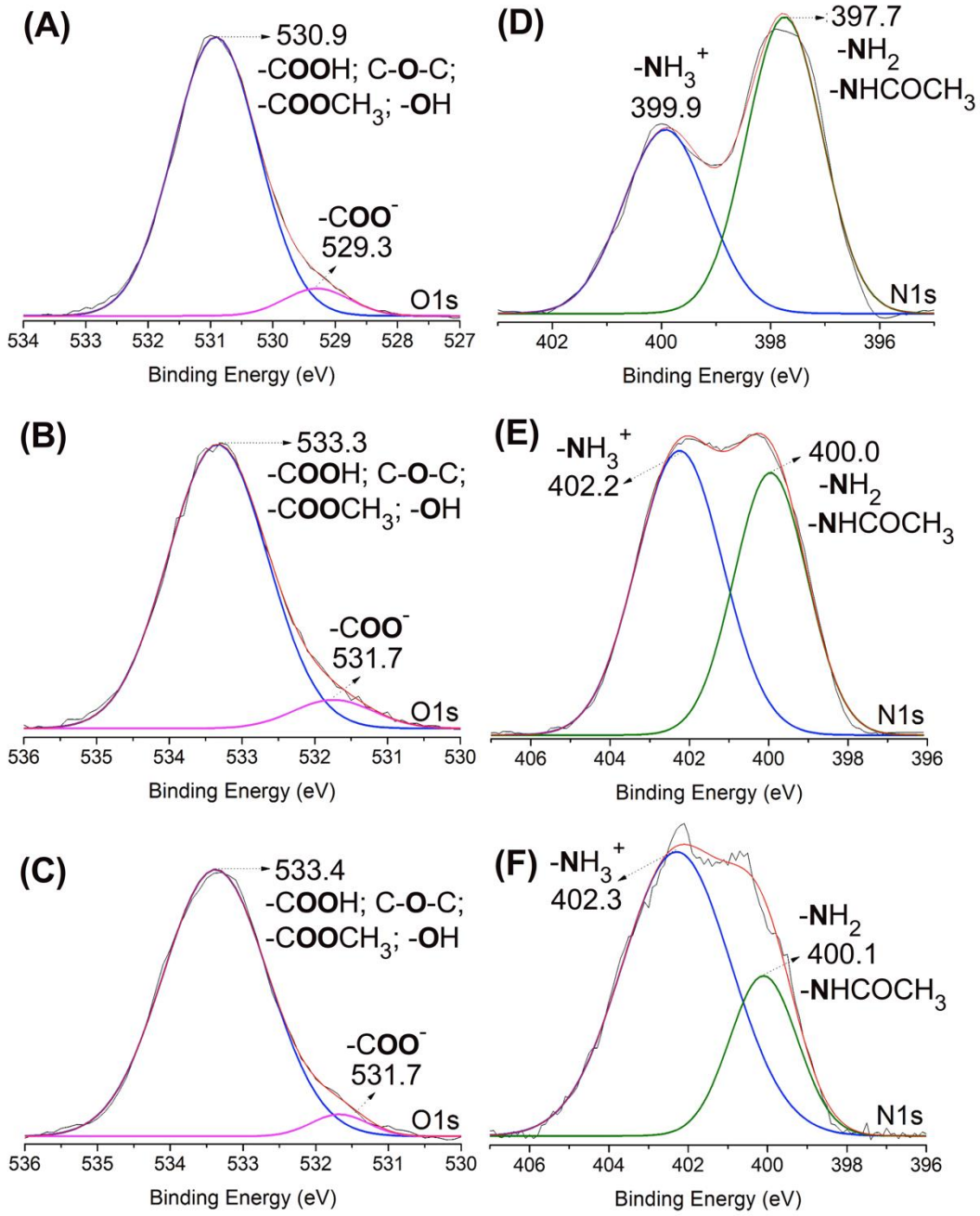

947

948 **Figure 8.** High-resolution XPS spectra (O1s and N1s) determined from cross-sections of the
949 neutralized hydrogel PECs: (A and D) CS/GG(80-20), (B and E) CS/GG(60-40), (C and F) CS/GG(50-
950 50).

951 The characteristic chemical groups of the CS and GG macromolecules, such
952 as $–NH_3^+$, $–NH_2$, $–COO^–$, –COOH, –COOR (R = $–CH_3$ or $–CH_2$-CH_3) and –OH, are
953 identified (Fig. 8). The electrostatic interactions between $–NH_3^+$ (on CS) and $–COO^–$
954 (on GG) sites comprise long-range forces in the neutralized CS/GG hydrogels. Also,
955 the high level of non-ionized chemical sites (–OH, $–NH_2$, and –COOH) imparts short-
956 range forces (intermolecular interactions) between polymer chains. Therefore,

957 neutralized CS/GG hydrogel structures are established by electrostatic interactions
958 between polysaccharide segments and intermolecular forces among polysaccharide
959 networks.

960 The relative percentages of $–NH_3^+$ and $–COO^–$ were also determined from
961 the peak areas, using each high-resolution XPS spectrum (Fig. 8). All hydrogels are
962 neutralized at least pH 5.8. This pH condition is much closer to the $–NH_2$ pK_a value
963 (6.5) than the –COOH pK_a (3.5). Therefore, slight changes in the pH around 5.8 can
964 significantly alter the $–NH_3^+$ relative percentage (Table 3). Besides, the $–COO^–$
965 relative percentages are low and comparable among the samples (Table 3). The
966 H_3O^+ excess of the CS solution should stabilize the double helix transition of GG
967 segments **(DE SOUZA et al., 2016)**, diminishing the ionization degree of the GG
968 chains during the neutralization, and reducing the amounts of $–COO^–$ sites in the
969 PECs (Table 3). However, the relative percentage of $–NH_3^+$ decreases when the
970 concentration of CS is raised (Table 3). In a high CS concentration, there is
971 insufficient GG to stabilize the CS chains. Therefore, to minimize the repulsion effect
972 in the CS/GG(80-20) the relative amount of NH_3^+ is reduced (Table 3). Free $–NH_2$
973 sites can establish effective intermolecular interactions (H-bonds) to stabilize the
974 PEC structures.

975 The $–COO^–/–NH_3^+$ ratios in the hydrogel matrices were determined from the
976 high-resolution XPS spectra using the peak areas for $–COO^–$ site at 529-531 eV and
977 $–NH_3^+$ group at 399-403 eV (Fig. 8 and Table 3). Using the area values, we showed
978 that CS/GG(50-50) displayed the highest $–COO^–/–NH_3^+$ ratio (ca. 3.0), while the
979 other samples presented ratios of approximately 1.0. During the neutralization, the
980 self-assembling of polymer chains should minimize the repulsion in the system. The
981 repulsion is diminished when the $–COO^–/–NH_3^+$ ratio is close to 1.0. However, the
982 excess of negative charge density in the neutralized CS/GG(50-50) should impart
983 lower stability. This result agrees with the findings of degradation determined in PBS
984 after 14 days. In PBS, the GG chains are fully ionized, increasing the interaction with
985 water molecules and raising the degradation rate. All the XPS peak signals reported
986 in the survey and high-resolution XPS spectra here agree with other published
987 results **(GOVINDARAJ et al., 2017; ROMERO et al., 2015)**.

988 2.3.3.2. Scanning electron microscopy and self-assembling property

989 Fig. 9 shows SEM images of the lyophilized and neutralized CS/GG PECs
990 acquired after purification in water.

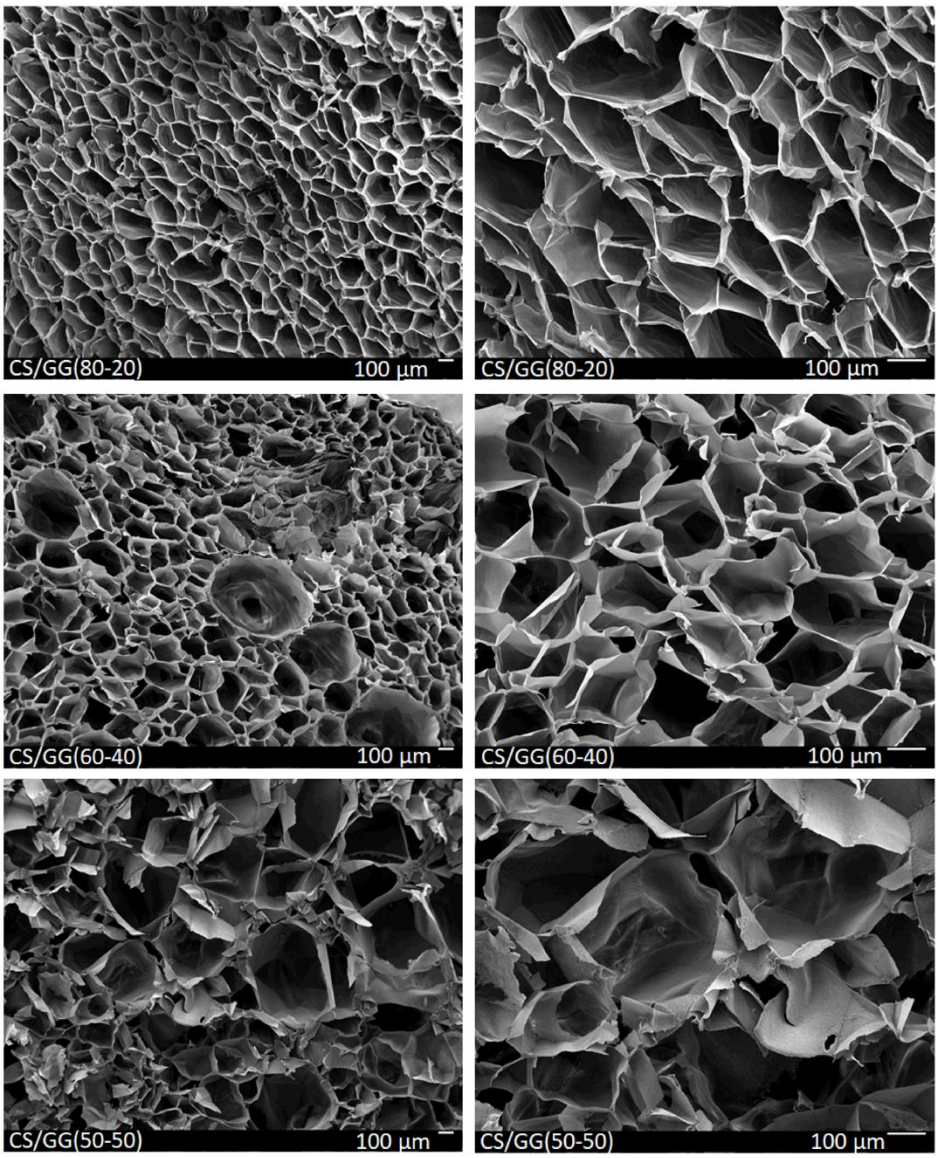

991

992 **Figure 9.** SEM images of the neutralized CS/GG hydrogels.

993 SEM analysis of the unneutralized and neutralized hydrogels (cross-sections
994 of the dried PECs prepared by fracturing) can explain why $–COO^-$/$–NH_3^+$ ratios
995 obtained in high-resolution XPS spectra are close to 1.0, even under CS excess
996 (wt.%) in the CS/GG(80-20) and CS/GG(60-40) structures. The CS/GG(80-20) and
997 CS/GG(60-40) have homogeneous assemblies with well-defined pores. The

998 neutralization of the samples promotes self-assembling of polymer chains,
999 increasing the homogeneity and porosity.

1000 Fig. 10 shows SEM images of the unneutralized CS/GG(60-40) and
1001 CS/GG(80-20) PECs. These samples showed brittle structures without pores. After
1002 neutralization, the reorganization of polymer chains (self-assembling) leads $–COO^-$/–
1003 NH_3^+ ratio to 1.0, increasing the stability and homogeneity. On the other hand, the
1004 neutralized CS/GG(50-50) hydrogel comprises a more brittle structure without well-
1005 defined pores (Fig. 9). The $–COO^-$/$–NH_3^+$ ratio is approximately 3.0 in the CS/GG(50-
1006 50) network, imparting a non-homogeneous structure because of the excess of
1007 negative charge density. These results agreed with the XPS and degradation
1008 (performed in PBS) findings.

1009 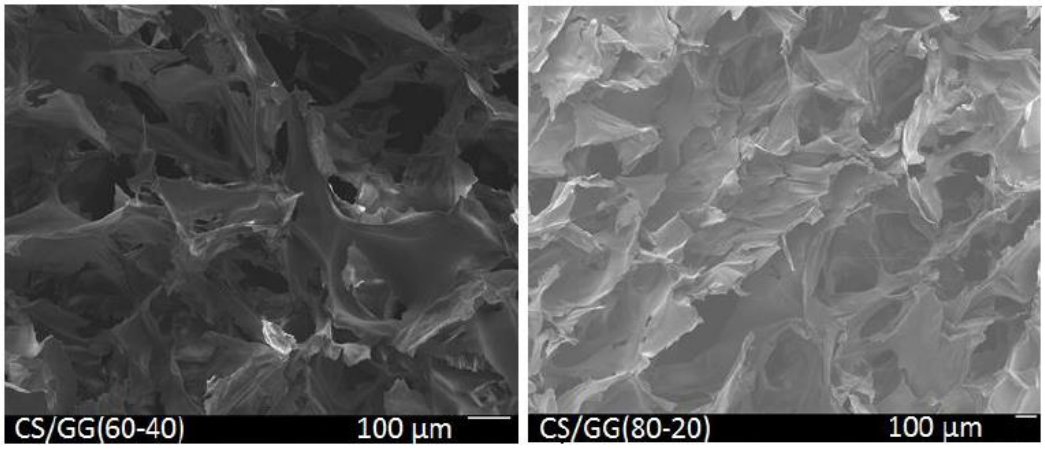

1010 **Figure 10.** SEM images of unneutralized PECs: CS/GG(60-40) (A) and CS/GG(80-20) (B).

1011 Depending on the CS/GG weight ratio, super-porous materials were created
1012 from CS/GG assembling. This finding also agreed with other results already reported
1013 in the literature. Neutralized CS/chondroitin sulfate PECs prepared at 40/60
1014 CS/chondroitin sulfate weight ratio also displayed stability and a large content of
1015 pores in its structure **(FAJARDO et al., 2010; PIAI; RUBIRA; MUNIZ, 2009)**.
1016

1017 2.3.3.3. Thermal analysis and self-assembling property

1018

1019 Thermal analysis was used to confirm the self-assembling property among
1020 CS and GG functional groups established after neutralization/washing step. DSC and

TGA/DTG curves of the polymer precursors are presented in Fig. 11, while TGA/DTG profiles for the hydrogels are provided in Fig 12.

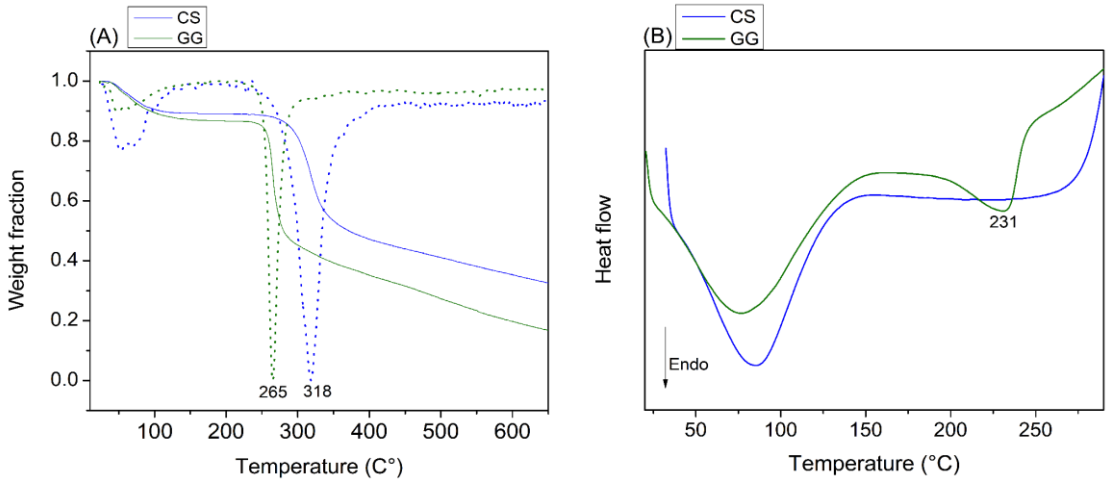

Figure 11. TGA/DTG (A) and DSC (B) curves of the chitosan (CS) and gellan gum (GG).

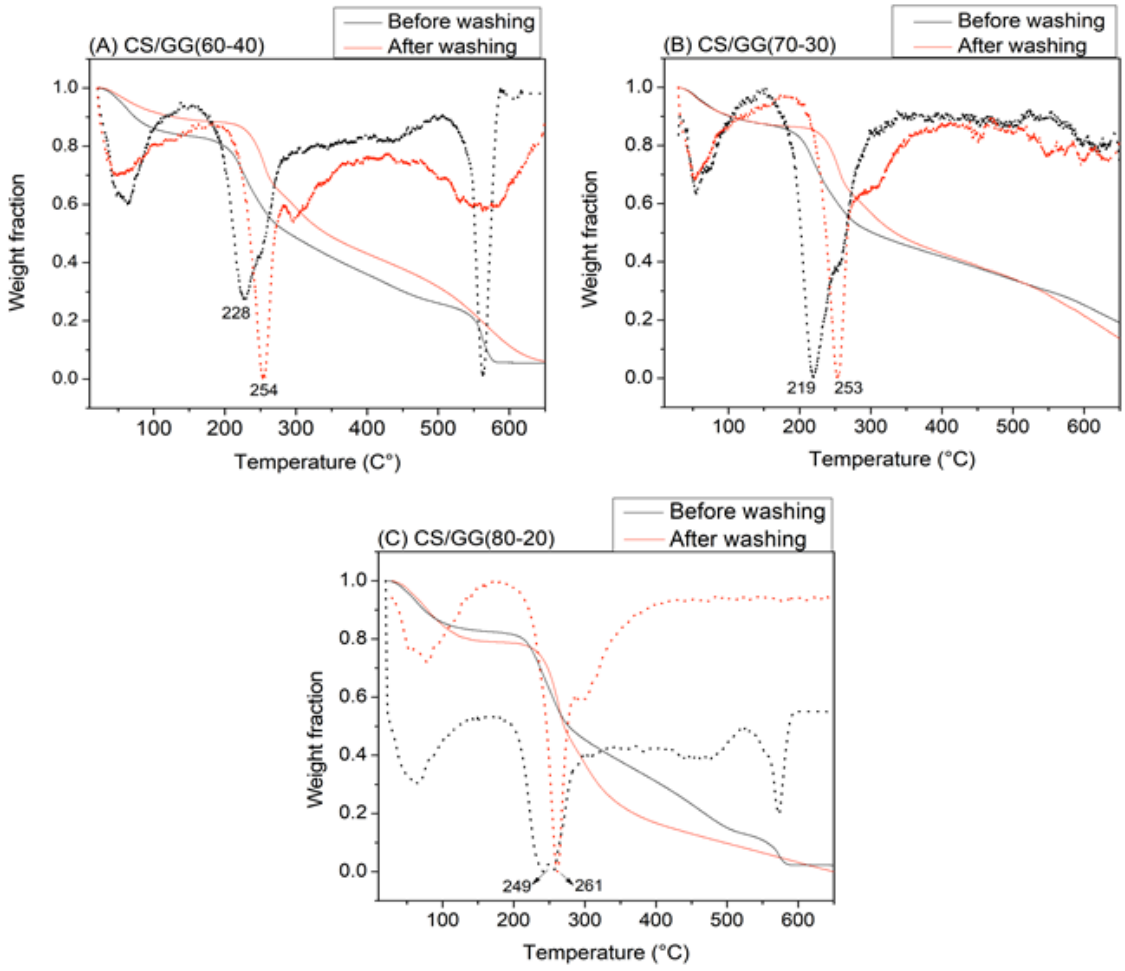

Figure 12. TGA/DTG curves of the neutralized and non-neutralized hydrogel PECs.

The TGA/DTG curves showed that CS had higher thermal stability than GG (Fig. 11A). DTG curves of GG and CS showed narrow and acute peaks at 265 and 318°C, respectively (Fig. 11A). The DSC curve of GG showed a broad endothermic peak at 231 °C, probably related to the melting temperature of semi-crystalline domains (Fig. 11B).

The TGA/DTG curves of the hydrogels illustrated at least four stages of mass loss (Fig. 12). The first event, between 50 and 150°C, corresponded to the loss of water and volatile compounds and represented a loss of mass in the range of 10 to 20%. The PECs showed similar water contents when compared to the pure CS and GG polysaccharides (Fig. 11A) due to the same storage conditions. The second and third events occurred between 200 and 400°C and the DTG curves showed inflection points in the range of 219 to 261°C (Fig. 12). The high temperatures attributed to the degradation events may be associated with the formation of favorable interactions between the CS and GG chains, established mainly after neutralization (after reorganization) of the PECs. In the range of 200 to 400°C, the degradation of the PECs resulted in approximately 40 to 50% mass loss (Fig. 12). All thermal events in this range were mainly attributed to pyrolytic decomposition, associated with primary and secondary decarboxylation of the polymer chains **(GORRASI; BUGATTI; VITTORIA, 2012)**. In the range of 500 to 650°C oxidation of by-products occurred. However, this thermal stage should appear late in some cases **(GORRASI; BUGATTI; VITTORIA, 2012).** Compared to the thermal analysis results presented in this study, profiles of DSC and TGA/DTG curves of pectin/CS based PECs showed similar behavior **(MARTINS et al., 2018b)**.

The DSC curves of the hydrogels are shown in Figure 13. The DSC curves of the non-neutralized PECs have wider endothermic peaks occurring in the range of 211 to 214ºC, while the DSC profiles of the neutralized PECs exhibit narrower endothermic peaks in the region of 222 to 224°C (Fig. 13). The temperatures of the endothermic peaks in the DSC curves of the neutralized PECs were higher with respect to the endothermic peak temperatures of the DSC curves of the unneutralized PECs. This indicates that upon neutralization, the polymer chains interact more efficiently in the neutralized materials. Neutralization promotes reorganization of the polymer networks due to a gradual change of pH throughout the neutralization step. Reorganization of polymer chains played a significant role in the

properties of hydrogels. Prior to neutralization, the CS chains were fully protonated and, after neutralization, they were partially deprotonated, inducing self-assembling of the polymeric chains in the PEC structures.

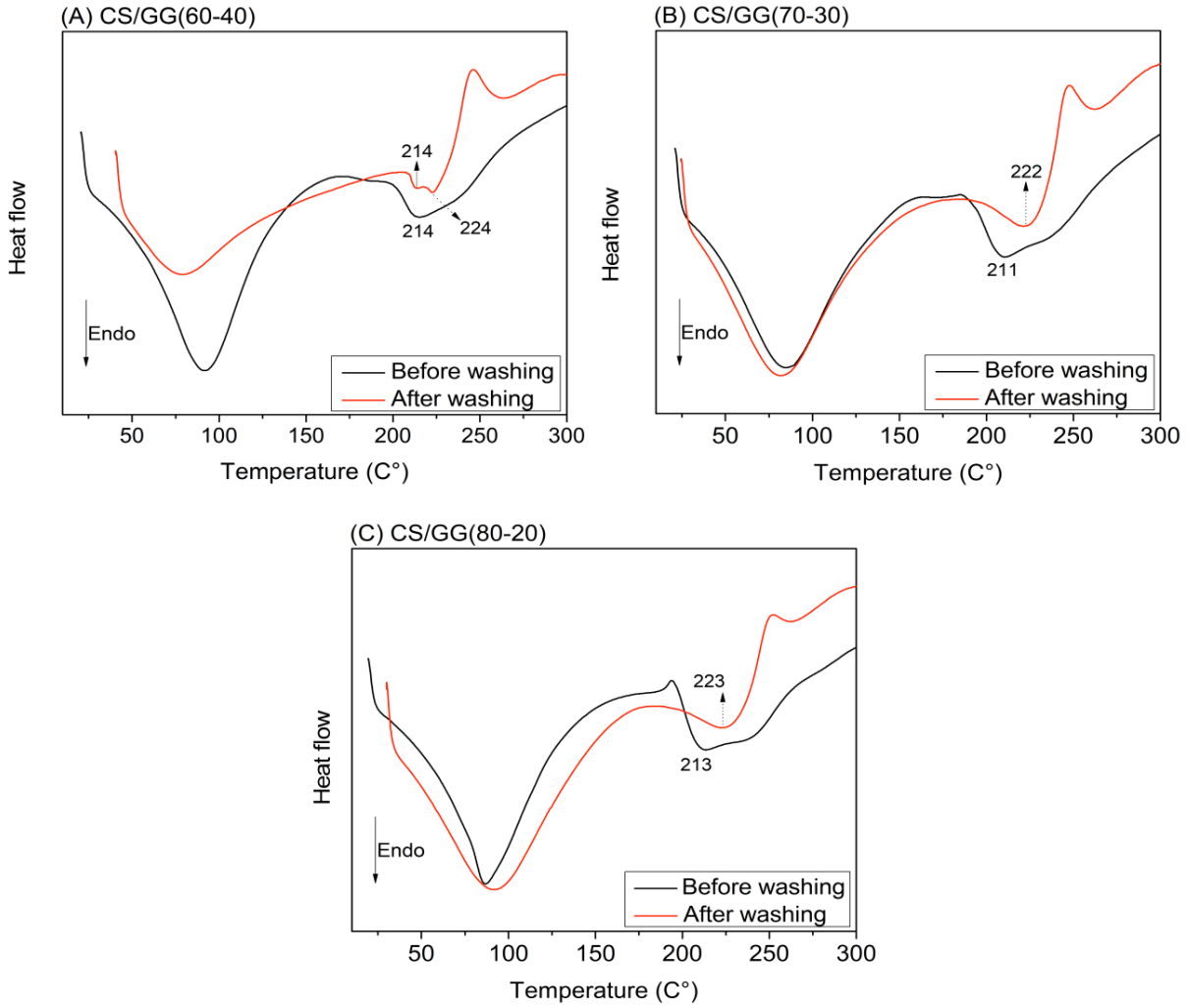

Figure 13. DSC curves of the neutralized and unneutralized hydrogel PECs.

2.4. CONCLUSIONS

CS/GG-based PECs can be created following a straightfoward procedure free of chemical processes and metallic ions as crosslinking agents. CS/GG PECs were formed by blending polymer solutions at 60°C, avoiding typical instability of polyelectrolytes mixtures, which often lead to precipitates. XPS analysis showed that PECs are created by the establishment of electrostatic and intermolecular

interactions between CS and GG chains. Tuning the CS/GG weight ratio we can develop durable PECs. The most water-stable PECs were obtained at the 60:40 CS:GG weight ratio. PECs were obtained with features of thermosensitivity, super-porosity, water stability and slow degradation rate in PBS and SGF media. These properties are imparted after self-assembling of the CS-GG polymer networks, confirmed by SEM and thermal analysis. All these properties make CS/GG PECs candidate materials for technological applications (medicine, pharmacy, agriculture, environmental and other arenas). Some of these potential applications will be investigated in future chapter.

CHAPTER 3: CHITOSAN/GELLAN GUM RATIO CONTENT IS MODULATED TO ENHANCE THE SCAFFOLDING CAPACITY OF POLYELECTROLYTE ASSEMBLIES

Abstract

Here, we have demonstrated the production and characterization of hydrogels based on chitosan and gellan gum (CS/GG) assemblies, without any covalent and metallic crosslinking agents, conventionally used to yield non-soluble polysaccharide-based materials. Hydrogels containing chitosan (CS) excesses (ranging from 60 to 80 wt.%) are created, and CS/GG weight ratio can be modulated to promote structural homogeneities, with interconnecting pore networks, durable PEC assemblies with hydrophilicity-hydrophobicity properties suitable to act as scaffold platforms for cell culture. A cytocompatible CS/GG hydrogel yielded at 80/20 CS/GG ratio (CS/GG80-20) supported fixation, growth, and spreading of bone mesenchymal stem cells (BMSCs) after nine days of culture. This work presents for the first time that CS/GG hydrogels can be applied for tissue engineering purposes.

Keywords: Polysaccharides, Tissue Engineering, Mesenchymal Stem Cells, Cell Culture

3.1. INTRODUCTION

PECs can be applied as tridimensional scaffold devices, aiming application in tissue engineering field **(MARTINS et al., 2018a)**. Depending on the experimental conditions used to yield PECs, these can show durability, controlled degradation rates, high porosities, and homogeneous structures with interconnecting pore networks **(WANG; WEN; BAI, 2016)**. These properties lead PECs candidate materials to be used as scaffold matrices **(LÓPEZ-CEBRAL et al., 2017)**. Besides, PECs can have water-stability, even without chemical crosslinking agents (glutaraldehyde, epichlorohydrin, genipin, and others) in their compositions **(FACCHI et al., 2018b)**. When degraded or dissolved, chemical hydrogels may impart cytotoxicity to the system **(LÓPEZ-CEBRAL et al., 2017)**, or yet, relying on the chemical crosslinking stability, these materials may decrease or still may suppress the scaffold biodegradability **(MACIEL; YOSHIDA; FRANCO, 2015; MARTINS et al., 2018a)**.

Scaffolds must mimic the extracellular membrane functions, such as the establishment of tissue microenvironments, sequestration, storage of regulatory-soluble molecules, mechanical support for cell anchorage, control of cell growth and proliferation, determination of cell orientation, transport of nutrients to guarantee the cell survival, and other functions **(FACCHI et al., 2017a; NAAHIDI et al., 2017)**. LÓPEZ-CEBRAL et al., (2017), have shown that physical GG-based scaffolds associated with endogen molecules and growth factor (BMP-2) acted as bone formation platforms **(LÓPEZ-CEBRAL et al., 2017)**, while CS/pectin PECs have supported the attachment, growth and spreading of adipose mesenchymal stem cells (AMSCs) **(MARTINS et al., 2018a)**. CS and GG can be associated to yield PECs with scaffolding performance; however, such capacity was not evaluated yet.

Following an unpublished methodology, CS/GG PECs are developed from aqueous CS/GG blends, tuning the CS/GG weight ratios. CS/GG PECs with great stabilities against the dissolution process in water, structural homogeneities, and high porosities are prepared by modulating the CS/GG weight ratios. The scaffolding capacity of the hydrogels was assessed on bone mesenchymal stem cells (BMSCs) after 4 and 9 days of cell culture. The ability to promote adhesion, proliferation and

spreading of BMSCs were determined by scanning electron microscopy (SEM) and fluorescence images. Hydrogel PECs were characterized through infrared spectroscopy (FTIR), wide-angle X-ray scattering (WAXS), and scanning electron microscopy (SEM). Also, properties such as *in vitro* degradation rate (using dried hydrogel samples) and swelling capacity of the dried PECs were evaluated after 4 and 9 days in PBS.

3.2. MATERIALS AND METHODS

KELCOGEL® gellan gum (GG) of low acyl degree and molar weight between 2.0 to 3.0×10^5 g mol^{-1} was graciously donated by CP Kelco Co., Limeira-SP (Brazil) **(PRAJAPATI et al., 2013)**. Chitosan (CS) with deacetylation degree of 85% and average molar weight of 87×10^3 g mol^{-1} was purchased from Golden-Shell Biochemical (China) **(FACCHI et al., 2018b)**.

3.2.1. Hydrogel preparation

The aqueous solution of CS (1.0 wt.%/vol.%) was prepared in dilute aqueous HCl solution (pH≈1.0), while the aqueous solution of GG (1.0 wt.%/vol.%) was obtained in deionized water (pH≈6.0). Both solutions were yielded by dissolving the polysaccharides at 60°C for 10 min. For obtaining PECs, aliquots of the GG-solution (1.0 wt.%/vol.% at 60°C) are slowly dropped into suitable aliquots of the CS-solution (1.0 wt.%/vol.% at 60°C) (Table 4). After dropping, the system is maintained under magnetic stirring for 5.0 min to form homogeneous CS/GG solutions. Then, flasks (10 mL) containing CS/GG blends (6.0 mL) were conditioned in a water bath at 25°C for 2.0 h to promote the physical crosslinking. Hydrogels were removed from the flasks and soaked in 50 mL deionized water under mild magnetic stirring. Aqueous NaOH solution (0.010 mol L^{-1}) was slowly dropped into the system to raise the pH to at least 5.8. After neutralization, all samples were frozen and lyophilized (-50°C for 72 h).

Table 4. Experimental conditions used to create CS/GG PECs.

Samples	CS (mL:g)	GG (mL:g)	CS:GG ratio[a]
CS/GG(80-20)	4.8:0.048	1.2:0.012	80:20
CS/GG(60-40)	3.6:0.036	2.4:0.024	60:40

[a]Weight ratio

3.2.2. Characterization

Fourier-transform infrared spectroscopy (FTIR) spectra were recorded using a Fourier transform infrared spectrophotometer (Shimadzu Scientific Instruments, Cary 630 Model), operating from 650 to 4000 cm^{-1}, at a resolution of 4 cm^{-1}, obtained after accumulating 64 scans. WAXS profiles were recorded on a Shimadzu diffractometer, model XRD-600, Japan equipped with a Ni-filtered Cu-Kα radiation. The WAXS profiles were collected in a scattering range (2θ) from 5° to 70°, with resolution of 0.02°, at a scanning speed of 2° min^{-1}. The analyses were performed by applying an accelerating voltage of 40 kV at 30 mA. This analysis was carried out at Maringá State University (Brazil).

The surface morphology of the dried hydrogel PECs was investigated through SEM. For obtaining the SEM images, samples were sputter-coated with palladium-gold alloy (Polaron SC 7620 Sputter Coater, Quorum Technologies, Newhaven, UK) at a thickness of 10 nm (10‑15 mA, under a vacuum of 130 mTorr). The SEM (JSM-6500F, field emission scanning electron microscope, JEOL, Japan) was operated at an accelerating voltage of 5 kV, and 3 to 6 locations on each sample were imaged. The average size of pores on hydrogel PEC surfaces was determined using the ImageJ software and SEM images at 100 μm of scale bar (10 counts). The SEM analysis was carried out at Colorado State University (CSU), USA.

3.2.3. *In vitro* degradation test

The initial dry weight (Wdry-I) of the hydrogel was immediately measured after lyophilization. Then, the dried hydrogel (approximately 0.1 g) was immersed in PBS (50 mL) and incubated at 37°C with shaking (100 rpm) **(CHEN et al., 2010)**. At

desired time intervals (after 4 and 9 days), the hydrogel was removed from the PBS buffer, dried (as described above) and weighed to evaluate the final dry weight (Wdry–F). The remaining weight (%) was determined using the following Equation

$$Remaining\ weight\ (\%) = \frac{Wdry - F}{Wdry - I} \times 100 \qquad (2)$$

3.2.4. Swelling assays

The swelling degree (SD) of the dried PECs was determined at 37ºC after contact with PBS (pH 7.4), using the Equation 2 **(NUNES et al., 2017b)**. This assay was performed after 4 and 9 days.

$$SD\% = \frac{Ws - Wd}{Wd} \times 100 \qquad (3)$$

Where the *Ws* and *Wd* are the weights of swollen and dried hydrogels, respectively. All the assays were performed in duplicate.

3.2.5. Cell culture and proliferation assays

3.2.5.1. Isolation of bone marrow stromal cells

Bone mesenchymal stem cells (BMSCs) were isolated from male Wistar rats (*Rattus norvegicus*) **(RUCKH et al., 2010)**. The animals were supplied by Harlan Sprague Dawley, Inc. (separate time points, unmixed cell populations). The animal protocol was approved by the Colorado State University Animal Care and Use Committee. This Committee complies with the NIH (National Institutes of Health) Guide for Care and Use of Laboratory Animals. Limbs were aseptically removed from recently killed animals, and soft tissue was removed from the bones. Metaphyseal end of the bones was removed to expose the bone marrow cavity. In a 50 mL conical tube, marrow was repeatedly flushed with culture medium (α-Minimum Essential Medium (α-MEM) with 10% fetal bovine serum (FBS, Sigma) and 1.0% penicillin/streptomycin (Sigma-Aldrich), using 10 mL syringes with 18 and 25-gauge

needles. Media containing cells and debris was filtered with a 70 mL nylon filter into a clean tube, and the cells were counted using a hemocytometer before seeding.

3.2.5.2. Cytocompatibility assay

Before BMSCs seeding, dried hydrogel PECs (samples of approximately 8×4 mm) were added to a 48-well plate and incubated in a sterilized PBS for 30 min under exposure to ultraviolet irradiation. Then, the PBS was removed, and the BMSCs (500 μL) were seeded on the samples at a density of 0.5 million well^{-1}. Cultures were incubated at 37°C under 5% CO_2 for 4 days **(RUCKH et al., 2010)**. Then, cell viability was determined by a CellTiter-Blue® cell viability assay (Alamar Blue assay, Promega G808A, Madison, WI), according to the manufacturer's instructions. After four days, 50 μL of CellTiter-Blue dye was added to sterilized hydrogel samples (CS/GG(60-40) and CS/GG(80-20), containing 500 μL culture media and they were incubated for 4 h at 37°C and 5% CO_2. Then, the supernatant absorbance was read in a microplate reader (Molecular Devices Spectra Max M3, Sunnyvale, CA) at 570 nm and 600 nm. The values of AlamarBlue reduction percentage (%AB) depend on the number of viable cells, i.e., the %AB correlates with the magnitude of dye reduction and is expressed as percentage of cell viability **(AL-NASIRY et al., 2007)**. The %AB reduction was corrected for background values of negative controls containing medium without cells and samples (AlamarBlue was added to medium without cells). To eliminate differences of %AB promoted by the cell culture medium, and then normalize the cell viability results (%), the experiment was repeated using culture media containing cells (0.5 million well^{-1}) and titanium foils (8×4 mm). One of the most commonly used bone substitute materials, the titanium sample was chosen as positive control due to its biomedical potential for implants and its renewed cytocompatibility **(DE VITERI; FUENTES, 2013)**.

3.2.5.3. Adhesion and proliferation tests

The BMSCs cell responses to the PEC hydrogels CS/GG(80-20) and CS/GG(60-40) were investigated after 4 and 9 days of culture in growth media. Cell adhesion and proliferation were appraised by staining the cells with rhodamine-

phalloidin to visualize the cytoskeleton, using a fluorescence microscope (Zeiss). Before staining, the media was aspirated, and the substrates were rinsed once in PBS before being transferred to a new 48-well plate where the cells were fixed at 3.7 vol.%/vol.% formaldehyde solution for 15 min at room temperature. The fixative was aspirated, and the substrates were rinsed thrice with PBS for 5 min before being transferred to a new 48-well plate. The cells were permeabilized at 1.0 vol.%/vol.% triton-X solution for 3 min at room temperature. The permeant was aspirated, and the substrates were rinsed and transferred to a new 48-well plate where they were incubated at 37°C in 5% CO_2 in a 5.0 µL mL^{-1} rhodamine-phalloidin solution for 25 min at 25°C. The remaining solution was aspirated, and the substrates were rinsed twice with PBS before being stored in PBS in a light resistant container at 20°C.

3.2.5.4. Cell morphology

SEM was used to compare the attachment and morphology of cells on the PEC hydrogels. As described before, after four and nine days of cell culture, the samples containing the attached BMSCs were fixed in a solution based on 3.7 vol.%/vol.% glutaraldehyde, 0.10 mol L^{-1} sodium cacodylate, and 0.10 mol L^{-1} sucrose for 45 min. Then, the samples were soaked for 10 min in a buffer solution of 0.10 mol L^{-1} sodium cacodylate and 0.10 mol L^{-1} sucrose. After, the PECs containing the cells were processed in serial ethanol dehydration for 10 min each and dehydrated in hexamethyldisilazane before being stored in a desiccator until imaging by SEM. The SEM images were obtained following the same conditions described before.

3.2.6. Statistical analysis

The results were statistically analyzed using ANOVA and Tukey tests at a 5% significance level (GraphPad Prism 6.0).

3.3. RESULTS AND DISCUSSION

3.3.1. Hydrogel formation

Fig. 14 depicts digital images of CS/GG blend at 60°C (Fig. 14A), unneutralized CS/GG assembly created at 80/20 CS/GG weight ratio (25°C) (Fig. 14B) and neutralized CS/GG(80-20) hydrogel (Fig. 14C). Stable assemblies are yielded at CS/GG weight ratios ranging from 80/20 to 60/40. CS/GG PECs have not produced above 90% CS concentration, because of the cationic polymer excess. GG polymer chains can be stabilized by cationic CS macromolecules **(SABADINI; MARTINS; PAWLICKA, 2015)**, and consequently by H_3O^+ ions **(DE SOUZA et al., 2016)** also provided in a dilute CS acid solution. When CS content is from 80 to 60 wt.%, CS/GG hydrogels are produced. However, raising the GG content to 50% (decreasing the H_3O^+ and CS contents), non-homogenous hydrogel structure is obtained, while at 60%, the hydrogel PEC is not stable during the washing step, and above 60% no assemblies are created. Therefore, the H_3O^+ and charged CS macromolecules can stabilize the GG chain segments to produce double-helix configurations and hence stable CS/GG assemblies. However, the CS/GG ratio needs to be fixed at 60/40 to 80/20 range to impart suitable CS and H_3O^+ concentrations to yield CS/GG assemblies after cooling of CS/GG blends (Fig. 14).

Panhuis and coworkers reported the formation of CS/GG PEC films by dipping free-standing films of either GG or CS into solutions of opposite charge **(AMIN; PANHUIS, 2011)**. It was shown that PEC production depended on pH and the order in which the biopolymers were added, i.e., soaking CS film into GG solution, or dipping GG film into CS solution **(AMIN; PANHUIS, 2011)**. Here, for obtaining PECs, GG-solution must slowly be dropped into the CS-solution. Otherwise, no stable CS/GG blends are formed.

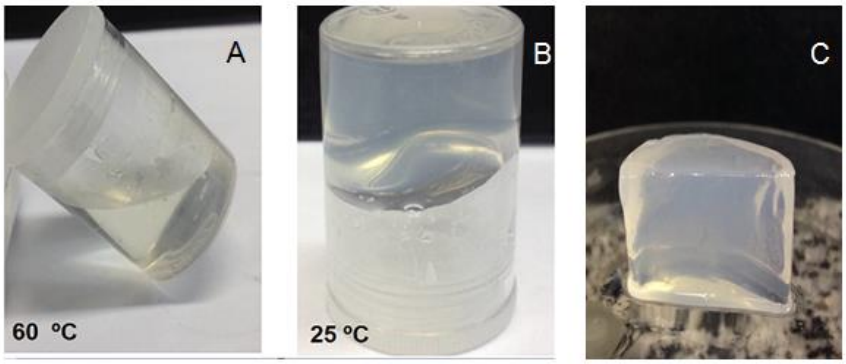

Figure 14. Digital images of the CS/GG blend at 60°C (Fig. 14A), unneutralized CS/GG(80-20) at 25°C (Fig. 14B) and neutralized CS/GG(80-20) hydrogel (Fig. 14C).

3.3.2. Characterization of the PECs through FTIR

Fig. 15 shows FTIR spectra of the CS (i), GG (ii) (Fig. 15A) and CS/GG assemblies (i and ii) (Fig. 15B).

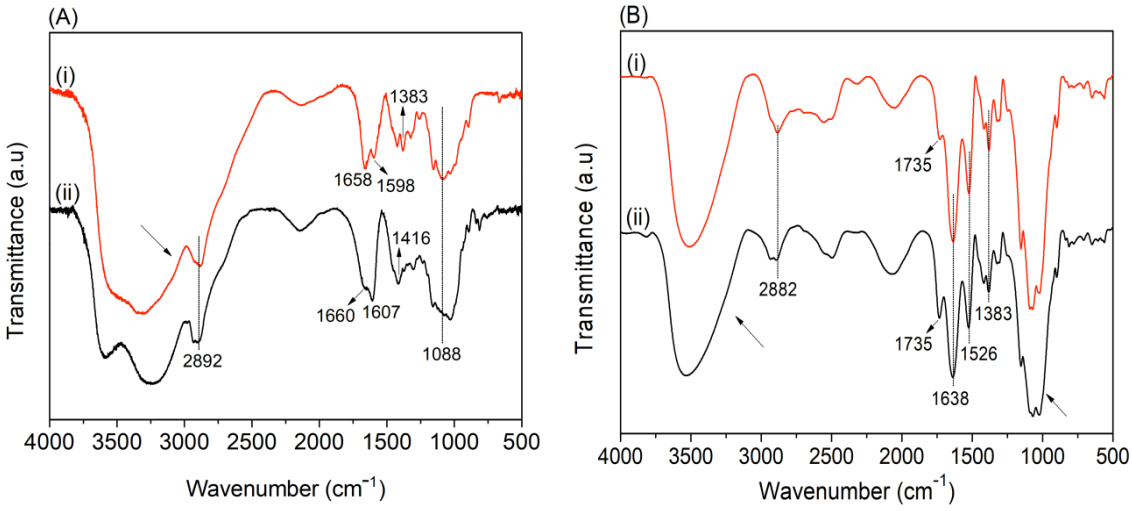

Figure 15. FTIR spectra: (A) CS (i) and GG (ii); (B) CS/GG(80-20) (i) and CS/GG(60/40) (ii).

CS FTIR spectrum presents characteristic bands at 1383, 1598 and 1658 cm^{-1} assigned to the –C–H bonds on $–NHCOCH_3$, –N–H stretching vibrations, and –C=O groups of amide sites, respectively (Fig. 15A(i)) **(NUNES et al., 2017)**. GG FTIR spectrum displays symmetric and asymmetric –C=O stretching vibrations at 1416

and 1607 cm^{-1} attributed to the carboxylate anions, sequentially; and –C=O absorption at 1660 cm^{-1} ascribed to the acylated moieties (Fig. 15A(ii)) **(SABADINI; MARTINS; PAWLICKA, 2015)**.

Characteristic bands on CS and on GG FTIR spectra have suffered alterations in the hydrogel FTIR spectra (Fig. 15B). The band at 1383 cm^{-1} remains in both PEC FTIR spectra, confirming the CS presence, while the band at 1526 cm^{-1} is assigned to the $-^{+}N-H$ bonds, indicating that CS and GG are interacting by coulombic forces on hydrogel matrices (Fig. 15B). CS/GG assemblies were created blending dilute acid CS solutions and GG solutions prepared in deionized water. The acid condition allows the partial protonation of the amine moieties on CS (pK_a = 6.5) and carboxylate anions on GG (pk_a = 3.5). Martins et al. have related similar results for obtaining CS/pectin PEC membranes **(MARTINS et al., 2018a)**.

These statements are corroborating with the band at 1638 cm^{-1} mostly related to the –C=O bonds of carboxylate anions and characteristic band at 1735 cm^{-1} ascribed to the –C=O of carboxylic acid moieties (–COOH groups) on GG chains **(BALASUBRAMANIAN; KIM; LEE, 2018; MARTINS et al., 2018b)**. The band at 1735 cm^{-1} is more intense on CS/GG(60-40) FTIR spectrum (Fig. 15B(ii)) because of the high GG content (40 wt.%). Compared to the CS and GG FTIR spectra, CS/GG PEC FTIR spectra had more narrow and sharp bands in the region between 3000 and 3600 cm^{-1} ascribed to the –O–H and –N–H bonds. In the PEC structures, CS and GG should interact by coulombic and intermolecular interactions. These rearrangements can destabilize the interactions among CS-CS and GG-GG polymer chain segments, conferring the spectral differences related before. Also, the band at 2892 cm^{-1} (assigned to the –C–H bonds) on precursor FTIR spectra (Fig. 15A) changed to 2882 cm^{-1} on PEC FTIR spectra (Fig. 15B) **(MARTINS et al., 2011)**. Another alteration has occurred on the spectral range (1088 cm^{-1}) assigned to the –C–O stretching of primary alcohols **(MARTINS et al., 2011)**. All these modifications have confirmed the formation of CS/GG-based PECs.

3.3.3. Characterization of the PECs through WAXS

Fig. 16 shows WAXS profiles of the CS (i), GG (ii) and CS/GG assemblies. CS WAXS profile exhibited two broad diffraction peaks at 2θ = 12.4° and 23.1°, which

confirmed the presence of semi-crystalline domains. These crystalline regions are attributed to the establishment of H-bonds between chain segments on CS polymer backbones **(MARTINS et al., 2013)**. However, the GG WAXS profile displayed two more broad diffraction peaks (2θ = 11.3° and 23.6°) than CS WAXS pattern because the GG predominantly comprises an amorphous structure **(XU et al., 2007)**. CS/GG(80/20) and CS/GG(60/40) WAXS patterns present two broad diffraction peaks at 2θ = 13.2° and 23.6°. Of note is that CS/GG(80-20) (iii) and CS/GG(60-40) (iv) WAXS profiles are slightly different from the GG WAXS profile. The GG should destabilize the H-bond interactions among CS-CS networks to form disorganized CS/GG assemblies. These statements agreed with the FTIR results. WAXS patterns of chondroitin sulfate/chitosan and heparin/N,N-dimethyl chitosan PECs already reported in the literature presented similar behaviors for their WAXS patterns when compared to the findings here demonstrated **(BUENO et al., 2015; NUNES et al., 2017b)**.

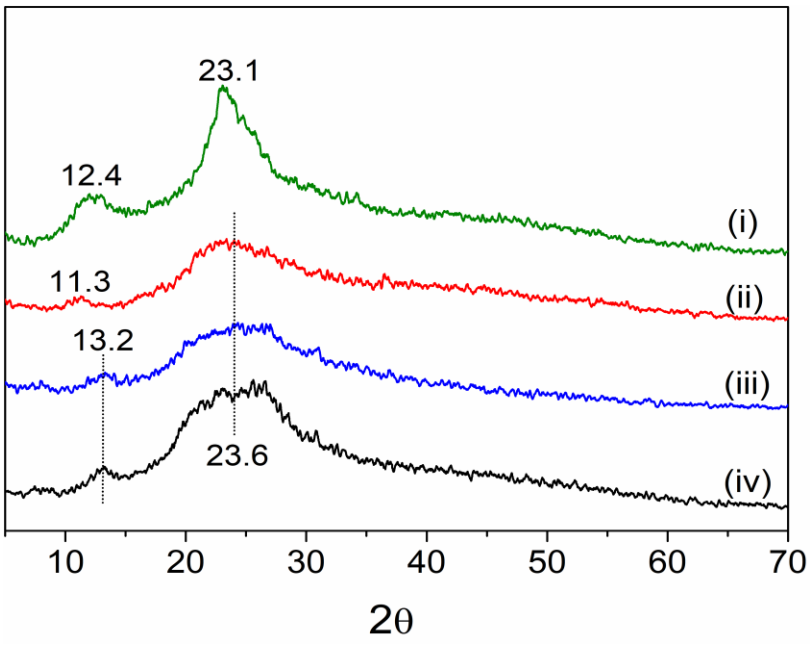

Figure 16. WAXS profiles: CS (i), GG (ii), CS/GG(80-20) (iii) and CS/GG(60-40).

3.3.4. Characterization of the PECs through SEM

Fig. 17 shows SEM images of the CS/GG assembly cross-sections. By adjusting the CS/GG ratio, materials with homogeneous structures, containing

defined and interconnected pore networks are developed (Fig. 17). The average size of pores on dried CS/GG(80-20) and CS/GG(60-40) cross-sections were 148±34 and 180±55 μm, respectively. Biomaterials with structural uniformity and high porosity (average size of pores ranging from 100 to 200 μm) are desired properties for scaffolds because they can mimic the ECM functions, such as transport of metabolites, as well as transport, migration, proliferation, differentiation of cells and ECM regeneration **(FREYMAN; YANNAS; GIBSON, 2001)**. The scaffolding capacity of CS/GG PECs will be demonstrated here. Our results have agreed with other current published findings. Kolanthai et al. developed PEC composites based on CS, alginate, collagen and graphene oxide with interconnecting pore networks with the mean size between 10 to 250 μm **(KOLANTHAI et al., 2018)**.

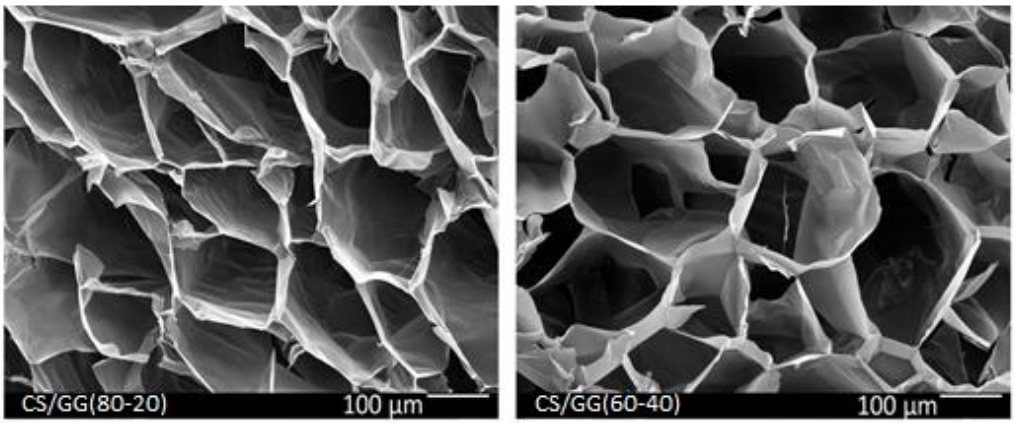

Figure 17. SEM images of the samples CS/GG(80-20) (A) and CS/GG(60-40) (B).

3.3.5. *In vitro* degradation and swelling assays

Results of degradation and swelling determined after 4 and 9 days in PBS (37ºC) are presented in Fig. 18. Dried CS/GG(80-20) containing the higher CS concentration (80 wt.%) showed great stability against degradation and slight humidity retention (Fig. 18A). This hydrogel showed no degradation within 9 days, probably because of the low CS solubility in alkaline medium. The CS/GG(80-20) SDs% of 1813% and 1576% are achieved after 4 and 9 days, respectively (Fig. 18B). Considering the CS/GG(80-20) assembly, no significant results (p>0.05) were found for degradation and swelling outcomes (Fig. 18).

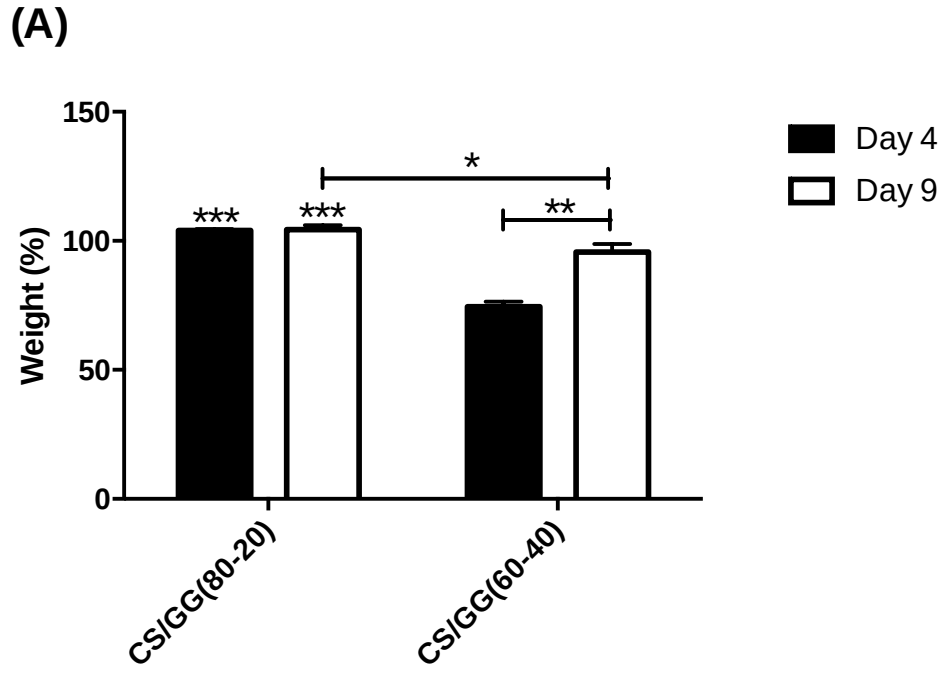

1398

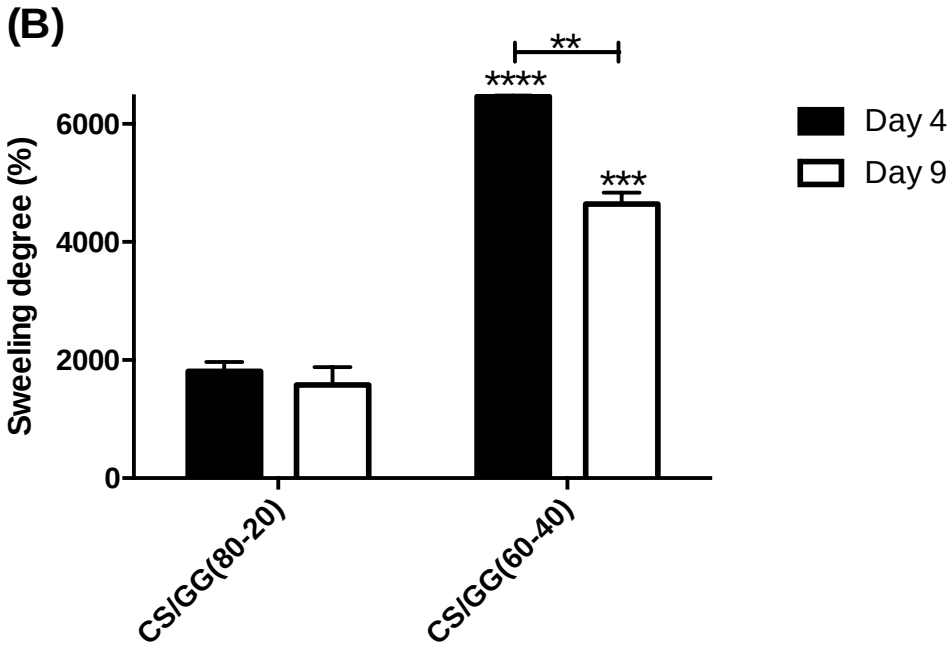

1399

1400 **Figure 18.** In vitro degradation results (A) and swelling degrees (B) of the hydrogels determined after
1401 4 and 9 days in PBS contact at 37ºC. The results have significant differences, where **** is indicating
1402 $p \leq 0.0001$, *** $p \leq 0.001$, ** $p \leq 0.01$ and * $p \leq 0.05$.

1403

1404 Overall, the CS/GG(60-40) PEC displayed higher degradation rates and
1405 swelling degrees because of the high GG content (40 wt.%) in its structure.
1406 Significant results of degradation and swelling were observed (at least $p \leq 0.05$; Fig.

18). Compared to CS, GG has more water solubility, and then high GG levels impart large water uptake for CS/GG(60-40) assembly (SD = 6460% in 4 days and 4646% in 9 days; Fig. 18B). This effect is maximized due to the presence of ionized $–COO^-$ sites on GG structure.

CS/GG(60-40) PEC prepared at 40 wt.% GG content degraded 25% (after 4 days) and only 5% (after 9 days) (Fig. 18A). Of note is that the degradation rate decreased after 4 days. This outcome should be associated with the self-assembling of the dried PEC chains in PBS. Fajardo et al. showed that dried CS/chondroitin sulfate PEC assemblies had presented self-reorganizing after contact with slight alkaline buffer solutions (pH 8.0) **(FAJARDO et al., 2010)**. This behavior was depending on both the swelling pH medium and swelling time **(FAJARDO et al., 2010)**. When applied, PEC-based scaffolds must be hydrophilic and have structural stability **(MARTINS et al., 2018a)**. These traits were achieved for the CS/GG assemblies; however, the cationic polymer concentration played a significant role in DS% and degradation outcomes (at least $p \leq 0.05$) because the CS excess (80 wt.%) in CS/GG(80-20) hydrogel significantly reduced the water uptake.

3.3.6. Cell viability assay

The BMSCs cell viability results promoted by the CS/GG(60-40), CS/GG(80-20) and titanium (positive control) are presented in Fig. 19. The titanium is one the most important material for bone replacement in biomedical applications **(DE VITERI; FUENTES, 2013)**. Therefore, it was chosen as a positive control due to its non-toxicity **(DE VITERI; FUENTES, 2013)**. Significant differences ($p \leq 0.01$) on the cell viability findings are observed concerning the cell viability (100%) promoted by the titanium. However, both hydrogels have imparted high values of cell viability (higher than 80%), even considering titanium as a positive control (Fig. 19).

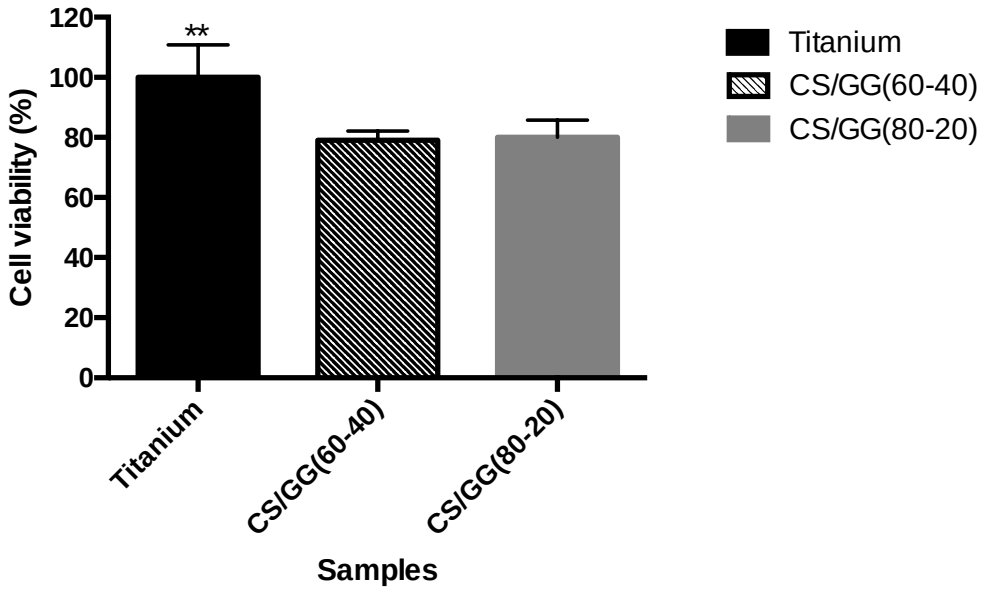

Figure 19. Cell viability results on the bone mesenchymal stem cells (BMSCs) after 4 days of cell culture represented as percentage reduction of AlamarBlue. Error bars indicate standard deviation (n = 5) and ** indicates $p \leq 0.01$. The titanium sample (8×4 mm) was used as positive control.

Therefore, CS/GG PECs are cytocompatible to BMSCs and can be useful candidates for biomedical applications. Such results agreed with other findings already reported. Bonifacio et al. have shown that GG/manuka honey hydrogels crosslinked by Ca^{2+} (0.025% w/v) and Mg^{2+} (0.50% w/v) under cationic physiological concentrations, also exhibited slight cell viability results than 80% on BMSCs **(BONIFACIO et al., 2018b)**. On the other hand, we have used the titanium foil samples to determine the normalized percentage of cell viability (100%), while Bonifacio and coworkers have applied an untreated control (cells without control sample) **(BONIFACIO et al., 2018b)**. In this case, the CS/GG PECs present high cytocompatibility even when compared with titanium (a renewed and cytocompatible material widely applied in the biomedical field).

3.3.7. Cell adhesion and proliferation

Fig. 20 shows SEM images of the hydrogels after cell culture assay seeded with BMSCs. In 4 days, the CS/GG(60-40) and CS/GG(80-20) hydrogels imparted similar morphologies when compared to the morphologies of the as-obtained materials (Fig. 20), confirming that PECs have appreciable stability in PBS. This buffer solution mimics the blood pH environment, i.e., the biological condition of living

organisms. After 4 days, both PEC matrices promoted cellular adhesion of BMSCs, as well as provided slight dissemination of such cells on their surfaces. Both samples have promoted similar results.

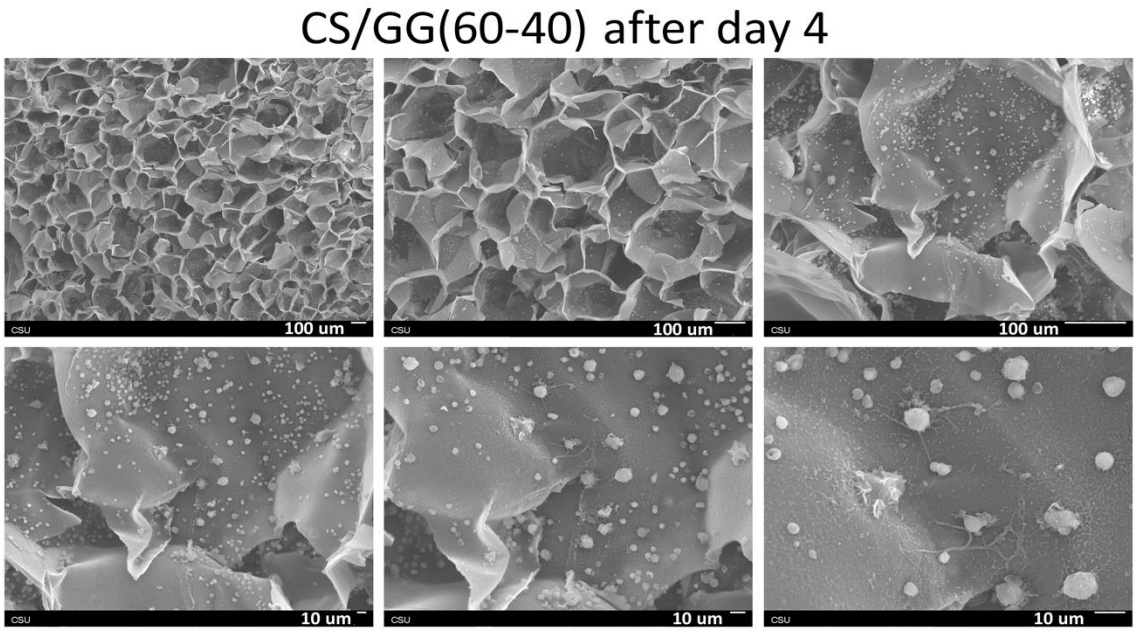

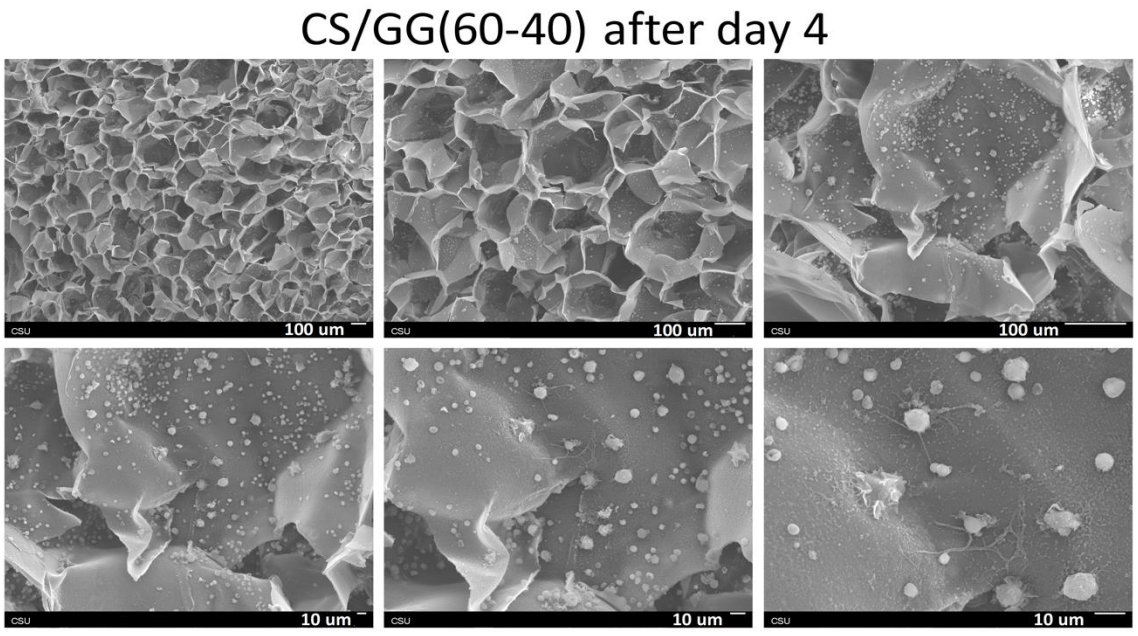

Figure 20. SEM images of BMSCs cells seeded on the hydrogel PECs after 4 days of cell culture.

On the other hand, after an extended period in PBS (after 9 days), PEC assemblies significantly exhibited different morphologies concerning the as-obtained materials, such as described in Fig. 20 (Fig. 21). A significant morphological change

took place on CS/GG(80-20) matrix because the blend prepared at CS/GG(80/20) ratio is further from the equimolar proportion. This effect should disrupt the maintenance of CS/GG(80-20) structure, even it containing 80 wt.% CS (a non-soluble polymer in PBS) (Fig. 21).

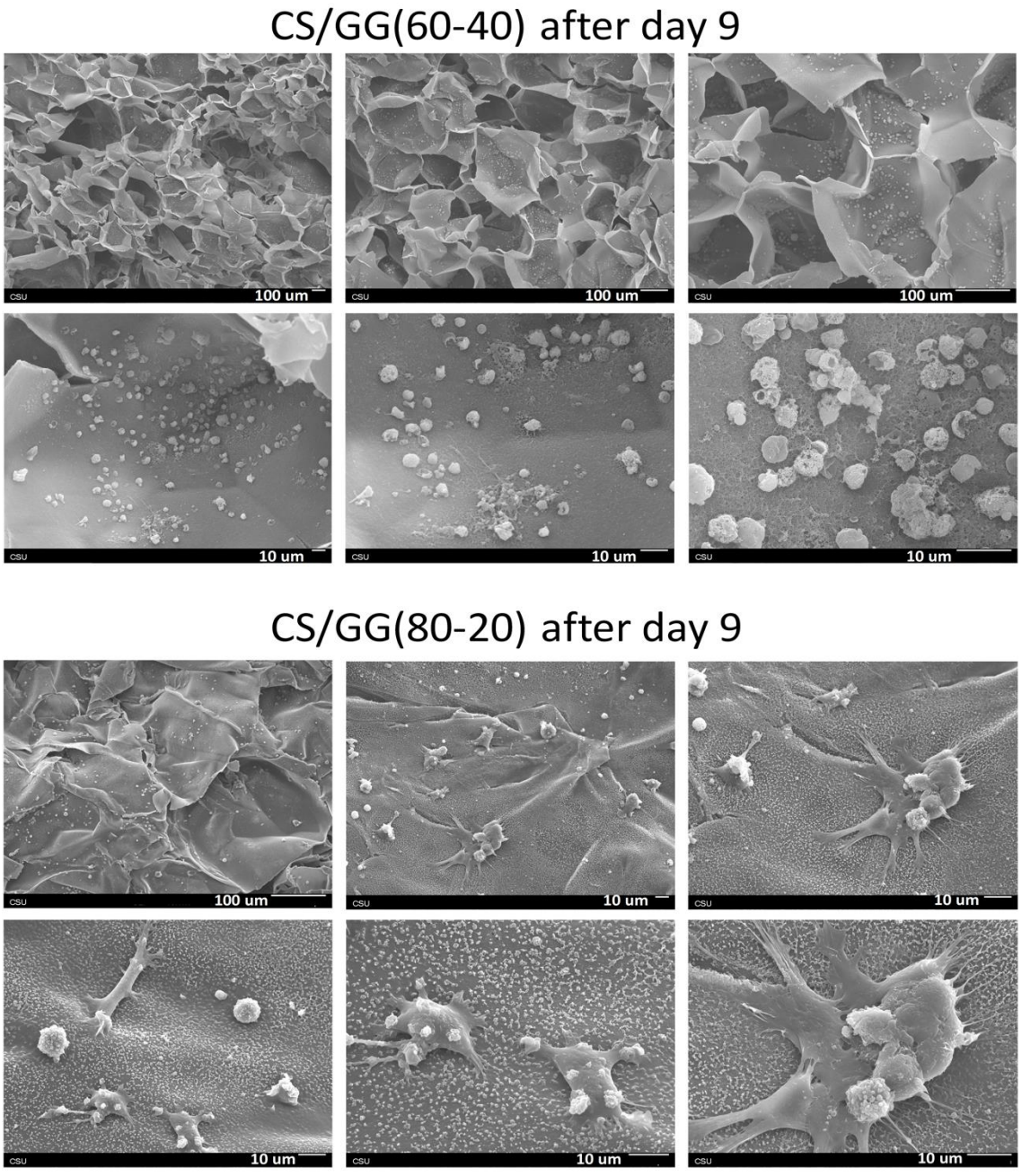

Figure 21. SEM images of BMSCs cells seeded on the hydrogel PECs after 4 and 9 days of cell culture.

Adjusting the CS/GG weight ratio, we can modulate the swelling capacity and hence the hydrophilic/hydrophobic property. In 9 days, CS/GG(80-20) assembly (SD = 1576%) showed excellent potential to promote dissemination of BMSCs than

CS/GG(60-40) PEC (DS = 4646%). The high-water uptake of the CS/GG(60-40) hydrogel, as well as the suitable GG wt.% should avoid the establishment of desirable microenvironments to foster BMSCs spreading and survival (Fig. 21). Martins et al. described similar results, which pectin/CS PEC (DS = 2416%) containing pectin excess (≈80 wt.%) did not promote adhesion, fixation, and dissemination of AMSCs after seven days of cell culture **(MARTINS et al., 2018a)**. On the other hand, the results for AMSCs survival and dissemination were achieved decreasing the pectin content to 66 wt.% in the pectin/CS assembly **(MARTINS et al., 2018a)**. So, CS should enhance the biological responses in the PEC-based scaffolds.

Fluorescence images of the hydrogels seeded with BMSCs (in 9 days of culture) confirmed the SEM data.

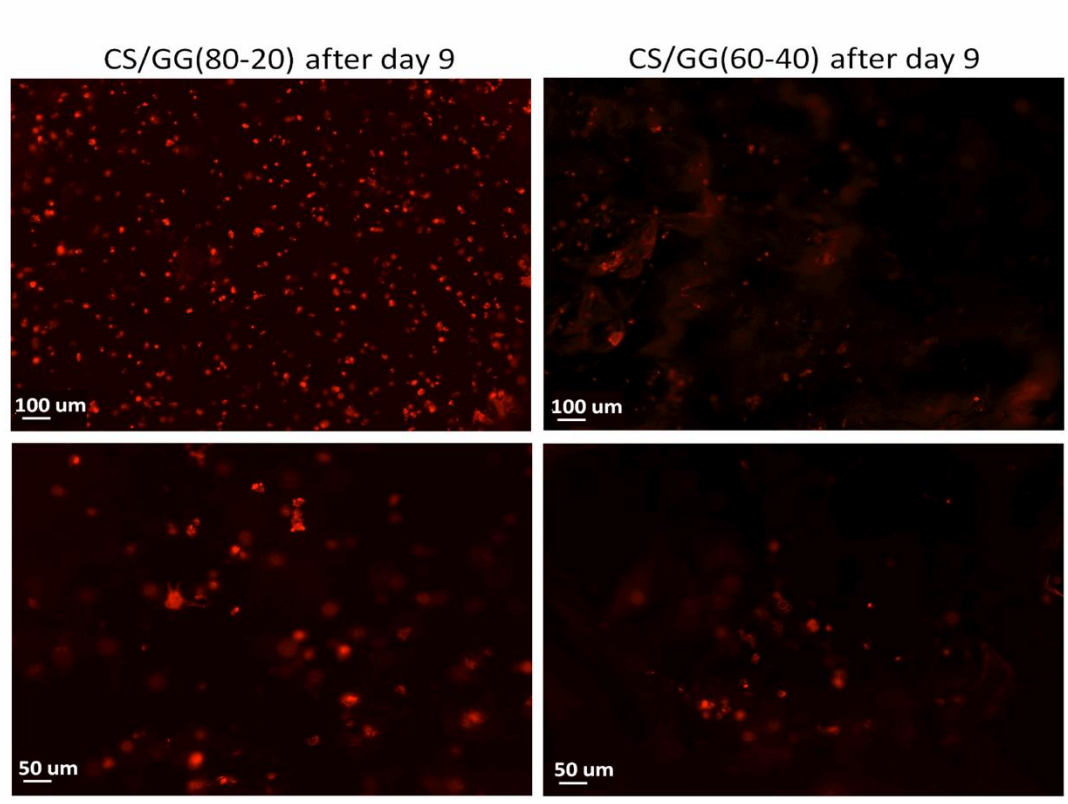

Figure 22. Representative fluorescent images of BMSCs on hydrogel PEC surfaces after 9 days of cell culture.

The cytoskeleton of cells is identified by rhodamine-phalloidin through red color (Fig. 22). After 9 days, the CS/GG(80-20) assembly has promoted greater adhesion, proliferation, and dissemination of BMSCs. Both hydrogels are durable in

PBS; however, only the CS/GG(80-20) PEC was appropriate to act as scaffold support. The spreading of BMSCs on CS/GG(80-20) surface should occur to form new tissues, stimulating processes of healing and repair **(DE SOUZA COSTA-JÚNIOR; PEREIRA; MANSUR, 2009)**. The attachment, proliferation, and dissemination of cells on scaffolds depend on the surface traits, including hydrophilicity/hydrophobicity and polarity **(BOMBALDI DE SOUZA et al., 2018)**. Cells have negative charge densities on ECM; therefore, a high GG content should suppress the BMSCs attachment and survival.

3.4. CONCLUSION

This study showed for the first time that a CS/GG assembly (free of any chemical and metallic crosslinking agent) could promote scaffolding capacity on bone mesenchymal stem cells (BMSCs). However, the higher GG content (higher than 20 wt.%) on PEC assembly has suppressed dissemination and survival of BMSCs. The CS/GG(80-20) PEC created at 80/20 CS/GG ratio imparted attachment, proliferation, and dissemination of BMSCs after 9 days of cell culture. By adjusting the CS/GG blend composition, we can modulate the hydrophilicity-hydrophobicity, allowing interactions between BMSCs and CS/GG(80-20) surface, obtaining desired biological responses. In particular, the CS/GG(80-20) biomaterial based on GG and GG polysaccharides can act as a scaffold for tissue engineering purposes.

CHAPTER 4: FINAL CONSIDERATIONS AND FUTURE PERSPECTIVES

PECs-based on gellan gum and chitosan were yielded for the first time without typical precipitation of polyelectrolytes in solution. Following a new experimental methodology and tuning the CS content to 80 wt.%, it was prepared a hydrogel PEC with cytocompatibility, hydrophilicity, stability, homogenous porosity, and scaffolding capacity onto bone mesenchymal stem cells (BMSCs). The CS/GG(80-20) promoted adhesion, growth, and proliferation of BMSCs, being a candidate material for tissue engineering purposes. The other hydrogel samples can have other potential applications. These systems we are applying as adsorbent materials to treat wastewater contaminated with toxic metals and dyes, as well as

drug carrier matrices. Of note is that we already produced CS/GG PECs loaded with curcumin (a non-soluble drug which presents anti-inflammatory, antimicrobial and carcinogenic properties against several types of cancer). We intend to show that CS/GG PEC can act a drug carrier matrix for curcumin.

REFERENCES

AGNIHOTRI, S. A.; JAWALKAR, S. S.; AMINABHAVI, T. M. Controlled release of cephalexin through gellan gum beads: Effect of formulation parameters on entrapment efficiency, size, and drug release. **European Journal of Pharmaceutics and Biopharmaceutics**, v. 63, n. 3, p. 249–261, 2006.

AHMED, E. M. Hydrogel: Preparation, characterization, and applications: A review. **Journal of Advanced Research**, v. 6, n. 2, p. 105–121, mar. 2015.

AL-NASIRY, S. et al. The use of Alamar Blue assay for quantitative analysis of viability, migration and invasion of choriocarcinoma cells. **Human Reproduction**, v. 22, n. 5, p. 1304–1309, 2007.

AMIN, K. A. M.; PANHUIS, M. IN HET. Polyelectrolyte complex materials from chitosan and gellan gum. **Carbohydrate Polymers**, v. 86, n. 1, p. 352–358, 2011.

AZEVEDO, V. V. C. et al. Quitina e Quitosana: aplicações como biomateriais. **Revista Eletrônica de Materiais e Processos**, v. 2.3, p. 27–34, 2007.

BALASUBRAMANIAN, R.; KIM, S. S.; LEE, J. Novel synergistic transparent k-Carrageenan/Xanthan gum/Gellan gum hydrogel film: Mechanical, thermal and water barrier properties. **International Journal of Biological Macromolecules**, v. 118, p. 561–568, 2018.

BERGER, J. et al. Structure and interactions in chitosan hydrogels formed by complexation or aggregation for biomedical applications. **European Journal of Pharmaceutics and Biopharmaceutics**, v. 57, n. 1, p. 35–52, jan. 2004.

BOMBALDI DE SOUZA, R. F. et al. Mechanically-enhanced polysaccharide-based

scaffolds for tissue engineering of soft tissues. **Materials Science & Engineering C**, v. 94, p. 364–375, 2018.

BONIFACIO, M. A. et al. Antibacterial effectiveness meets improved mechanical properties: Manuka honey/gellan gum composite hydrogels for cartilage repair. **Carbohydrate Polymers**, v. 198, p. 462–472, out. 2018a.

BORDERÍAS, A. J.; SÁNCHEZ-ALONSO, I.; PÉREZ-MATEOS, M. New applications of fibres in foods: Addition to fishery products. **Trends in Food Science & Technology**, v. 16, n. 10, p. 458–465, out. 2005.

BUENO, P. V. A. et al. N,N-Dimethyl chitosan/heparin polyelectrolyte complex vehicle for efficient heparin delivery. **International Journal of Biological Macromolecules**, v. 75, p. 186–191, abr. 2015.

CALÓ, E.; KHUTORYANSKIY, V. V. Biomedical applications of hydrogels: A review of patents and commercial products. **European Polymer Journal**, v. 65, p. 252–267, 2015.

CHEN, P. H. et al. Novel chitosan-pectin composite membranes with enhanced strength, hydrophilicity and controllable disintegration. **Carbohydrate Polymers**, v. 82, n. 4, p. 1236–1242, 2010.

CORONATO, Rafael Machado e Silva. **EFEITO DA GOMA GELANA EM SISTEMAS AMIDOÁGUA E AMIDO-LEITE.** 2010. 81 f. Dissertação (Mestrado) - Curso de Ciências e Tecnologia de Alimentos, Universidade Estadual de Londrina, Londrina, 2010.

COUTINHO, D. F. et al. Microfabricated photocrosslinkable polyelectrolyte-complex of chitosan and methacrylated gellan gum. **Journal of Materials Chemistry**, v. 22, n. 33, p. 17262, jul. 2012.

DE SOUZA COSTA-JÚNIOR, E.; PEREIRA, M. M.; MANSUR, H. S. Properties and biocompatibility of chitosan films modified by blending with PVA and chemically crosslinked. **Journal of Materials Science: Materials in Medicine**, v. 20, n. 2, p. 553–561, 6 fev. 2009.

DE SOUZA, F. S. et al. Evaluation of different methods to prepare superabsorbent

hydrogels based on deacetylated gellan. **Carbohydrate Polymers**, v. 148, p. 309–317, set. 2016.

DE VITERI, V. S.; FUENTES, E. Titanium and Titanium Alloys as Biomaterials. In: **Tribology - Fundamentals and Advancements**. [s.l: s.n.].

DEWAN, M. et al. Effect of gellan gum on the thermogelation property and drug release profile of Poloxamer 407 based ophthalmic formulation. **International Journal of Biological Macromolecules**, v. 102, p. 258–265, 2017.

FACCHI, D. P. et al. Polysaccharide-based materials associated with or coordinated to gold nanoparticles: Synthesis and medical application. **Curr Med Chem**, v. 24, n. 25, p. 2701–2735, 2017a.

FACCHI, D. P. et al. Polyelectrolyte complexes based on alginate/tanfloc: Optimization, characterization and medical application. **International Journal of Biological Macromolecules**, v. 103, p. 129–138, out. 2017b.

FACCHI, D. P. et al. New magnetic chitosan/alginate/Fe3O4@SiO2 hydrogel composites applied for removal of Pb(II) ions from aqueous systems. **Chemical Engineering Journal**, v. 337, p. 595–608, abr. 2018a.

FACCHI, S. P. et al. Preparation and cytotoxicity of N-modified chitosan nanoparticles applied in curcumin delivery. **International Journal of Biological Macromolecules**, v. 87, p. 237–245, 2016.

FAJARDO, A. R. et al. Time- and pH-dependent self-rearrangement of a swollen polymer network based on polyelectrolytes complexes of chitosan/chondroitin sulfate. **Carbohydrate Polymers**, v. 80, n. 3, p. 934–943, 5 maio 2010.

FERNÁNDEZ-FERREIRO, A. et al. In vitro and in vivo ocular safety and eye surface permanence determination by direct and Magnetic Resonance Imaging of ion-sensitive hydrogels based on gellan gum and kappa-carrageenan. **European Journal of Pharmaceutics and Biopharmaceutics**, v. 94, p. 342–351, 2015.

FREYMAN, T. M.; YANNAS, I. V.; GIBSON, L. J. Cellular materials as porous scaffolds for tissue engineering. **Progress in Materials Science**, v. 46, n. 3–4, p. 273–282, 2001.

1612 GANTAR, A. et al. Nanoparticulate bioactive-glass-reinforced gellan-gum hydrogels
1613 for bone-tissue engineering. **Materials Science and Engineering C**, v. 43, p. 27–36,
1614 2014.

1615 GIAVASIS, I.; HARVEY, L. M.; MCNEIL, B. Gellan Gum. **Critical Reviews in**
1616 **Biotechnology**, v. 20, n. 3, p. 177–211, 2008.

1617 GORRASI, G.; BUGATTI, V.; VITTORIA, V. Pectins filled with LDH-antimicrobial
1618 molecules: Preparation, characterization and physical properties. **Carbohydrate**
1619 **Polymers**, v. 89, n. 1, p. 132–137, 2012.

1620 GOVINDARAJ, D. et al. Carbon nanotubes/pectin/minerals substituted apatite
1621 nanocomposite depositions on anodized titanium for hard tissue implant: In vivo
1622 biological performance†. **Materials Chemistry and Physics**, v. 194, p. 77–89, 2017.

1623 GUILHERME, M. R. et al. Superabsorbent hydrogels based on polysaccharides for
1624 application in agriculture as soil conditioner and nutrient carrier: A review. **European**
1625 **Polymer Journal**, v. 72, p. 365–385, 2015.

1626 HAJJI, S. et al. Structural analysis, and antioxidant and antibacterial properties of
1627 chitosan-poly (vinyl alcohol) biodegradable films. **Environmental Science and**
1628 **Pollution Research**, v. 23, n. 15, p. 15310–15320, 23 ago. 2016.

1629 HEDAYATI, M. et al. Nanostructured Surfaces That Mimic the Vascular Endothelial
1630 Glycocalyx Reduce Blood Protein Adsorption and Prevent Fibrin Network Formation.
1631 **ACS Applied Materials & Interfaces**, v. 10, n. 38, p. 31892–31902, 26 set. 2018.

1632 HOFFMAN, A. S. **Hydrogels for biomedical applicationsAdvanced Drug Delivery**
1633 **Reviews**Elsevier, , jan. 2002.

1634 HUANG, Z. et al. A novel biodegradable β-cyclodextrin-based hydrogel for the
1635 removal of heavy metal ions. **Carbohydrate Polymers**, v. 97, n. 2, p. 496–501, set.
1636 2013.

1637 INSUA, I.; WILKINSON, A.; FERNANDEZ-TRILLO, F. Polyion complex (PIC)
1638 particles: Preparation and biomedical applications. **European Polymer Journal**, v.
1639 81, p. 198–215, ago. 2016.

1640 KAMOUN, E. A.; KENAWY, E.-R. S.; CHEN, X. A review on polymeric hydrogel

membranes for wound dressing applications: PVA-based hydrogel dressings. **Journal of Advanced Research**, v. 8, n. 3, p. 217–233, maio 2017.

KIRCHMAJER, D. M. et al. Enhanced gelation properties of purified gellan gum. **Carbohydrate Research**, v. 388, n. 1, p. 125–129, 2014.

KOLANTHAI, E. et al. Graphene Oxide—A Tool for the Preparation of Chemically Crosslinking Free Alginate–Chitosan–Collagen Scaffolds for Bone Tissue Engineering. **ACS Applied Materials & Interfaces**, v. 10, n. 15, p. 12441–12452, 18 abr. 2018.

KUMAR, S. et al. Ketoconazole encapsulated in chitosan-gellan gum nanocomplexes exhibits prolonged antifungal activity. **International Journal of Biological Macromolecules**, v. 93, p. 988–994, 2016.

LIU, L. et al. Chitosan fibers enhanced gellan gum hydrogels with superior mechanical properties and water-holding capacity. **Carbohydrate Polymers**, v. 97, n. 1, p. 152–158, 2013.

LIU, L. et al. Thermal behavior and properties of chitosan fibers enhanced polysaccharide hydrogels. **Thermochimica Acta**, v. 583, p. 8–14, 2014.

LÓPEZ-CEBRAL, R. et al. Gellan gum based physical hydrogels incorporating highly valuable endogen molecules and associating BMP-2 as bone formation platforms. **Carbohydrate Polymers**, v. 167, p. 345–355, jul. 2017.

LUO, Y.; WANG, Q. Recent development of chitosan-based polyelectrolyte complexes with natural polysaccharides for drug delivery. **International Journal of Biological Macromolecules**, v. 64, p. 353–367, 2014.

MACIEL, V. B. V.; YOSHIDA, C. M. P.; FRANCO, T. T. Chitosan/pectin polyelectrolyte complex as a pH indicator. **Carbohydrate Polymers**, v. 132, p. 537–545, nov. 2015.

MARTINS, A. F. et al. Polyelectrolyte complexes of chitosan/heparin and N,N,N-trimethyl chitosan/heparin obtained at different pH: I. Preparation, characterization, and controlled release of heparin. **Colloid and Polymer Science**, v. 289, n. 10, p. 1133–1144, 17 jul. 2011.

MARTINS, A. F. et al. Characterization of N-trimethyl chitosan/alginate complexes and curcumin release. **International Journal of Biological Macromolecules**, v. 57, p. 174–184, 2013.

MARTINS, A. F. et al. Preparation and cytotoxicity of N,N,N-trimethyl chitosan/alginate beads containing gold nanoparticles. **International Journal of Biological Macromolecules**, v. 72, p. 466–471, 2015.

MARTINS, J. G. et al. Pectin-chitosan membrane scaffold imparts controlled stem cell adhesion and proliferation. **Carbohydrate Polymers**, v. 197, n. April, p. 47–56, 2018a.

MARTINS, J. G. et al. Durable pectin/chitosan membranes with self-assembling, water resistance and enhanced mechanical properties. **Carbohydrate Polymers**, v. 188, p. 136–142, 2018b.

MOHAMED, R. R.; ELELLA, M. H. A.; SABAA, M. W. Cytotoxicity and metal ions removal using antibacterial biodegradable hydrogels based on N -quaternized chitosan/poly(acrylic acid). **International Journal of Biological Macromolecules**, v. 98, p. 302–313, maio 2017.

MORE, S. M. et al. Glutaraldehyde-crosslinked poly(vinyl alcohol) hydrogel discs for the controlled release of antidiabetic drug. **Journal of Applied Polymer Science**, p. NA-NA, 2010.

MOURA, C. M. DE et al. Quitina e quitosana produzidas a partir de resíduos de camarão e siri: avaliação do processo em escala piloto. **VETOR - Revista de Ciências Exatas e Engenharias**, v. 16,1, p. 37–45, 2007.

NAAHIDI, S. et al. Biocompatibility of hydrogel-based scaffolds for tissue engineering applications. **Biotechnology Advances**, v. 35, n. 5, p. 530–544, 2017.

NUNES, C. S. et al. Chitosan/chondroitin sulfate hydrogels prepared in [Hmim][HSO 4] ionic liquid. **Carbohydrate Polymers**, v. 170, p. 99–106, ago. 2017.

OSMAŁEK, T.; FROELICH, A.; TASAREK, S. Application of gellan gum in pharmacy and medicine. **International Journal of Pharmaceutics**, v. 466, n. 1–2, p. 328–340, 2014.

1699 PIAI, J. F.; RUBIRA, A. F.; MUNIZ, E. C. Self-assembly of a swollen
1700 chitosan/chondroitin sulfate hydrogel by outward diffusion of the chondroitin sulfate
1701 chains. **Acta Biomaterialia**, v. 5, n. 7, p. 2601–2609, 2009.

1702 PICONE, C. S. F.; CUNHA, R. L. Chitosan-gellan electrostatic complexes: Influence
1703 of preparation conditions and surfactant presence. **Carbohydrate Polymers**, v. 94,
1704 n. 1, p. 695–703, 2013.

1705 PRAJAPATI, V. D. et al. An insight into the emerging exopolysaccharide gellan gum
1706 as a novel polymer. **Carbohydrate Polymers**, v. 93, n. 2, p. 670–678, 2013.

1707 RINAUDO, M. Chitin and chitosan: Properties and applications. **Progress in**
1708 **Polymer Science (Oxford)**, v. 31, n. 7, p. 603–632, 2006.

1709 ROMERO, R. et al. Coating cortical bone allografts with periosteum-mimetic scaffolds
1710 made of chitosan, trimethyl chitosan, and heparin. **Carbohydrate Polymers**, v. 122,
1711 p. 144–151, 2015.

1712 RUCKH, T. T. et al. Osteogenic differentiation of bone marrow stromal cells on
1713 poly(ε-caprolactone) nanofiber scaffolds. **Acta Biomaterialia**, v. 6, n. 8, p. 2949–
1714 2959, 2010.

1715 SABADINI, R. C.; MARTINS, V. C. A.; PAWLICKA, A. Synthesis and characterization
1716 of gellan gum: chitosan biohydrogels for soil humidity control and fertilizer release.
1717 **Cellulose**, v. 22, n. 3, p. 2045–2054, 17 jun. 2015.

1718 SALUNKE, S. R.; PATIL, S. B. Ion activated in situ gel of gellan gum containing
1719 salbutamol sulphate for nasal administration. **International Journal of Biological**
1720 **Macromolecules**, v. 87, p. 41–47, 2016.

1721 SAUL, J. M.; WILLIAMS, D. F. Hydrogels in Regenerative Medicine. **Handbook of**
1722 **Polymer Applications in Medicine and Medical Devices**, p. 279–302, 2013.

1723 SHUKLA, R. et al. Fabrication of Apigenin loaded gellan gum–chitosan hydrogels
1724 (GGCH-HGs) for effective diabetic wound healing. **International Journal of**
1725 **Biological Macromolecules**, v. 91, p. 1110–1119, 2016.

1726 TANG, Y. et al. An improved complex gel of modified gellan gum and carboxymethyl
1727 chitosan for chondrocytes encapsulation. **Carbohydrate Polymers**, v. 88, n. 1, p.

46–53, 2012.

TAVARIA, F. K. et al. A quitosana como biomaterial odontológico: estado da arte. **Revista Brasileira de Engenharia Biomédica**, v. 29, n. 1, p. 110–120, 4 abr. 2013.

TENTOR, F. R. et al. Scaffolds based on chitosan/pectin thermosensitive hydrogels containing gold nanoparticles. **International Journal of Biological Macromolecules**, v. 102, p. 1186–1194, 2017.

VILELA, J. A. P. et al. Preparation, characterization and in vitro digestibility of gellan and chitosan-gellan microgels. **Carbohydrate Polymers**, v. 117, p. 54–62, 2015.

WANG, F.; WEN, Y.; BAI, T. The composite hydrogels of polyvinyl alcohol–gellan gum-Ca2 + with improved network structure and mechanical property. **Materials Science and Engineering C**, v. 69, p. 268–275, 2016.

XU, X. et al. Characterization of konjac glucomannan-gellan gum blend films and their suitability for release of nisin incorporated therein. **Carbohydrate Polymers**, v. 70, n. 2, p. 192–197, 2007.

YU, I.; KAONIS, S.; CHEN, R. **A Study on Degradation Behavior of 3D Printed Gellan Gum Scaffolds**. Procedia CIRP. **Anais**...2017

ZEMMOURI, H. et al. Coagulation Flocculation Test of Keddara's Water Dam Using Chitosan and Sulfate Aluminium. **Procedia Engineering**, v. 33, p. 254–260, 2012.

ZHANG, L. et al. A composite hydrogel of chitosan/heparin/poly (γ-glutamic acid) loaded with superoxide dismutase for wound healing. **Carbohydrate Polymers**, v. 180, p. 168–174, jan. 2018.

ZHU, Y. et al. Collagen–chitosan polymer as a scaffold for the proliferation of human adipose tissue-derived stem cells. **Journal of Materials Science: Materials in Medicine**, v. 20, n. 3, p. 799–808, 20 mar. 2009.

ZIA, K. M. et al. Recent trends on gellan gum blends with natural and synthetic polymers: A review. **International Journal of Biological Macromolecules**, v. 109, p. 1068–1087, abr. 2018.